Proposal to Continue the Study of Direct CP Violation and Rare Decay Processes in KTeV in 1999

Dec. 9, 1997

E. Cheu, S.A. Taegar, J. Wang
University of Arizona, Tucson, Arizona 85721

E. Blucher, S. Bright, G. Graham, J. Graham, R. Kessler, E. Monnier [1], V. Prasad, A. Roodman, N. Solomey, B. Quinn, Y. Wah, B. Winstein, R. Winston, E. D. Zimmerman
The Enrico Fermi Institute, The University of Chicago, Chicago Illinois 60637

A. R. Barker, J. LaDue, P. Toale
University of Colorado, Boulder, Colorado 80309

E. C. Swallow
Department of Physics, Elmhurst College, Elmhurst, Illinois, 60126 and
The Enrico Fermi Institute, The University of Chicago, Chicago, Illinois 60637

L. Bellantoni, R. Ben-David, G. Bock, S. Childress, R. Coleman, M. B. Crisler, R. Ford, Y. B. Hsiung, D. A. Jensen, P. McBride, H. Nguyen, V. O'Dell, M. Pang, R. Pordes, E. Ramberg, R. E. Ray, P. Shanahan, R. Tschirhart, H. B. White, J. Whitmore
Fermi National Accelerator Laboratory, Batavia Illinois 60510

K. Arisaka, W. Slater, A. Tripathi
University of California at Los Angeles, Los Angeles, California 90095

K. Hanagaki, M. Hazumi, S Hidaka, M. Sadamoto, K. Senyo, T. Yamanaka
Department of Physics, Osaka University, Toyonaka, Osaka, 560 Japan

A. Bellavance, M. D. Corcoran
Rice University, Houston, Texas 77005

S. Averitte, J. Belz, D. R. Bergman, E. Halkiadakis, A. Lath, S. Schnetzer, S. Somalwar, R. J. Tesarek, G. B. Thomson
Rutgers University, Piscataway, New Jersey 08855

J. Adams, M. Arenton, G. Corti, B. Cox, A. Golossanov, A. Ledovskoy, K.S. Nelson, J. Shields
University of Virginia, Charlottesville, VA 22901

A. Alavi-Harati, T. Alexopoulos, A.R. Erwin, M. A. Thompson
University of Wisconsin, Madison, Wisconsin 53706

[1]On leave from C.P.P Marseille/C.N.R.S., France

SUMMARY

The KTeV collaboration proposes to carry out further studies of direct CP violation and other rare processes in neutral kaon decays at the Tevatron fixed target run in 1999. The recently concluded KTeV run in FY97 (KTeV97) consisted of two physics programs which address the most important issues currently accessible to the neutral kaon sector: a precise measurement of the direct CP violation parameter ϵ'/ϵ (E832), and a study of CP violating and other rare kaon decays (E799-II). The upcoming Tevatron run with the Main Injector (KTeV99), combined with the FY97 run, provides us with the opportunity to meet and perhaps exceed our original goals for both programs and to start on a new physics program for the future.

Our goals for the 1999 run are:

1. to double the statistics of the ϵ'/ϵ measurement;
2. to at least triple the statistics in rare kaon and hyperon decays;
3. to continue our studies of $K_L \to \pi^0\nu\overline{\nu}$, which will include the first KAMI prototype detectors operating in a realistic beam environment.

During the 1997 run, we collected 4 million $K_L \to 2\pi^0$ events corresponding to a statistical error of around 1.5×10^{-4} on ϵ'/ϵ. Ten weeks of running time in 1999 will allow us to double the 1997 data sample with improved systematics. Additionally, with a larger beam intensity and a longer spill length, at least a factor of three improvement in sensitivity can be achieved for all of the rare decay modes with an additional nine weeks of running time. Finally, we are planing to allocate one week of our running time to a special run optimized for the study of $K_L \to \pi^0\nu\overline{\nu}$. This study will be an important step towards a program to detect and measure this mode in KAMI.

Contents

List of Figures

List of Tables

1 Introduction

The origin of CP violation is one of the fundamental questions of particle physics. Since the first observation of CP violation in 1964, kaon physics has provided the only real window through which to observe this phenomenon. One of the best established methods for studying the origin of CP violation rests in the observation of both K_L and K_S decays into $\pi^+\pi^-$ and $2\pi^0$[1][2][3]. If the CKM matrix is indeed the source of CP violation, the parameter ϵ'/ϵ, derived from the double ratio of these decays, is expected to be non-zero.

Alternative approaches to the study of direct CP violation have received serious attention over the past decade[4]. According to the Standard Model, rare decay modes such as $K_L \to \pi^0 e^+ e^-$ and $K_L \to \pi^0 \mu^+ \mu^-$ have direct CP violating amplitudes which are comparable to or larger than their CP conserving and indirect CP violating amplitudes. In addition, the rare decay mode of $K_L \to \pi^0 \nu\overline{\nu}$ is a virtually pure direct CP violating decay with very small theoretical uncertainties. Observation of this mode would allow the cleanest determination of the height of the unitarity triangle, the parameter in the Standard Model which determines the size of all CP violating observables[5][6][7]. Currently, E799-I has achieved the best sensitivity to these modes (see references contained in Table 6).

The KTeV collaboration was formed with the goal of probing the most relevant questions relating to CP violation which are accessible via the neutral kaon system to levels which have not previously been attainable[8]. A new physics program to measure the value of ϵ'/ϵ with unprecedented precision ($\sigma = 1 \times 10^{-4}$) was approved as E832 in 1992 as the primary goal of the KTeV project. Two significant experimental efforts to measure ϵ'/ϵ with comparable precision over the next few years are also underway at CERN (NA48) and Frascati (KLOE). A program to investigate rare CP violating kaon decays, originally approved as E799 in 1988, evolved into another physics program in KTeV: E799-II. After several years of construction, the experiment was successfully commissioned in the summer of 1996.

The 1997 run of KTeV (KTeV97) is reviewed in Section 2. The physics program at the anticipated FY99 Fixed Target run (KTeV99) is proposed in Section 3 where the expected physics reach of the program is discussed in some detail. Section 4 contains a description of upgrades to the existing kaon beam line and the KTeV detector which are required in order to carry out the proposed program.

2 Status and Results From the 1997 KTeV Run

The KTeV experiment first ran with a hadron beam on August 31, 1996, about one year after the detector hall was completed. Following a brief period of commissioning and repairs, the experiment began to collect physics quality data by the end of October 1996. The one year run was divided into five periods (see Table 1), of which two were used for ϵ'/ϵ running (E832) and two for rare decays (E799).

In the following sections, we briefly summarize the performance of the detector during the 1997 run, and give the current status of data analysis for E832 and E799.

Date	Data-taking Mode
10/24/96 - 12/18/96	E832 (ϵ'/ϵ)
12/21/96	$K_L \to \pi^0 \nu \overline{\nu}$ special run
1/24/97 - 3/24/97	E799 (rare decays)
4/2/97 - 7/23/97	E832 (ϵ'/ϵ)
7/24/97 - 9/2/97	E799 (rare decays)

Table 1: Summary of KTeV 1997 Runs.

2.1 Beam and Detector Performance

Both the KTeV beam line and detector (see Fig. 1) represent significant improvements over previous experiments. Table 2 compares various parameters from the KTeV experiment with the best performance of this group's previous experiments at FNAL (E731, E773, E799).

The KTeV beam design was driven by the need for clean neutral beams for the E832 ϵ'/ϵ measurement. The E799 rare decay experiment also requires clean beams in order to achieve reasonable trigger rates with large beam fluxes. In addition to improved muon sweeping and filtering, the neutral beam halo was minimized by precise collimation and reduced detector material in the beam. This resulted in significantly less radiation damage to the CsI calorimeter and lower trigger rates.

The heart of the KTeV detector is the CsI calorimeter. The energy scale of the calorimeter is directly related to the reconstructed z position for neutral decays, and is therefore a critical part of understanding the detector's acceptance for neutral events. The ratio of energy measured in the calorimeter to the momentum measured in the spectrometer for a sample of electrons is shown in Fig. 2(a). A fit to this distribution gives $\sigma(E/p) = 0.76\%$. Note that this resolution includes a significant contribution from the momentum measurement. Figure 2(b) is a plot of $\sigma(E/p)$ vs. p after subtracting the uncertainty on the momentum measurement. Finally, Fig. 2(c) shows the linearity of the calorimeter's response. We believe that the energy resolution of this calorimeter is the best that has been achieved in our field. Figure 3 shows a typical online event display of a $K_L \to 2\pi^0$ decay.

The E731/E773/E799 drift chambers were restrung with aluminum cathode wires and equipped with new electronics for KTeV. The new electronics and wires resulted in improved reliability over what had been achieved previously. The momentum resolution of the charged spectrometer is improved compared to the previous experiments as a result of reduced multiple scattering (better vacuum, Al cathode wires, thinner chamber windows, better He bags) and the higher p_t kick of the new analysis magnet.

The 1.8 m long totally active regenerator, required by E832 to produce K_S decays, has reduced the inelastic background scattered from the regenerator to $\sim 0.3\%$ in the vacuum beam, a factor of 6 lower than in E731.

Transition Radiation Detectors (TRD) were constructed to enhance our π/e rejection for rare decays in E799. The TRD system consists of 8 large (2 m x 2 m) planar modules. Each module consists of a radiator and chambers filled with xenon gas. These detectors are rolled into the beam during E799 data-taking. The system performed well and provides

Parameter	E731/E773/E799	KTeV
Pressure in decay region	500 μTorr	1 μTorr
μ flux per proton on target	4×10^{-5}	2×10^{-7}
Max. proton flux/spill	2.0E12	5.0E12
Calorimeter radiation exposure (E799)	450 rad/E12/week	50 rad/E12/week
γ energy resolution at 20 GeV/c	3.5%	0.65%
calorimeter nonlinearity (3-75 GeV/c)	10%	0.4%
π/e rejection, calorimeter	$\sim$ 50	$\sim$ 400
Magnetic field (p_t kick)	200 MeV/c	400 MeV/c
Magnetic field nonuniformity	5%	1%
Material in spectrometer (rl)	$\sim$ 0.87%	$\sim$ 0.35%
Single wire plane resolution	$\sim$ 85μm	$\sim$ 100μm
Track momentum resolution at 20 GeV/c	0.5%	0.25%
2μ efficiency	82%	99%
Regenerator: Inelastic background in vac. beam	$\sim$ 1.8%	$\sim$ 0.3%
γ veto performance (p.e. / MeV)	0.02	0.2
π/e rejection, TRD system	NA	$\sim$ 150
Level 2 clustering-trigger time	30 μs	2 μs
Level 2 tracking-trigger time	3 μs	1.5 μs
Level 2 TRD-trigger time	NA	1 μs
Level 3 complete event reconstruction	NA	200k events/spill
DAQ output	$\sim$ 20 MB / spill	$\sim$ 300 MB/spill
Livetime	0.7 at 0.8E11 p/spill	0.7 at 3.5E12 p/spill
Offline $\pi^0\pi^0$ mass resolution (MeV/c^2)	5.5	1.6
Offline $\pi^+\pi^-$ mass resolution (MeV/c^2)	3.5	1.8

Table 2: Comparison between E731/E773/E799 and KTeV.

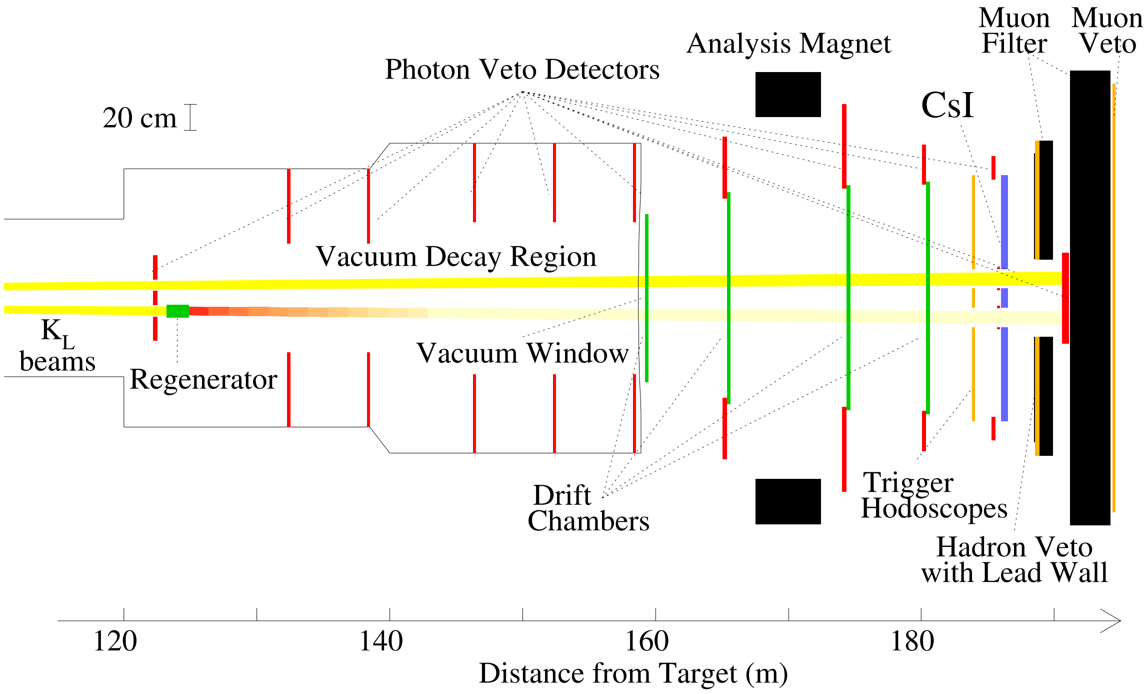

Figure 1: Plan view of KTeV detector (E832 configuration).

π/e rejection of better than 150:1 (for 90% electron detection efficiency) under typical E799 running conditions and has reached nearly 300:1 for some runs (see Fig. 4). A second level trigger processor used TRD information to provide π/e separation at trigger level.

The trigger and data acquisition system also performed well, providing vastly greater throughput with lower dead time than previous experiments. The data acquisition system also allowed us to monitor the performance of each detector subsystem, as well as various physics quantities. Early detection of problems using this system was critical to collecting high quality data.

Although the first KTeV run overall was quite successful, several difficulties were encountered which will be addressed for the 1999 run. These items, which are listed below, will be discussed in detail later in the proposal.

1. CsI Electronics. More than half of the beam time lost during the 1996-1997 run resulted from failures in the two custom integrated circuits used in the CsI calorimeter readout. The failures have been understood to result from fabrication problems at the IC vendor. The chips will be replaced for the 1999 run.

2. Drift Chamber System. The efficiency of the drift chamber system for detecting single drift electrons was lower in KTeV than in E731. This inefficiency resulted in anomalously long drift times for tracks passing close to a sense wire, and resulted in a bias in our 1996 data sample (see Section 2.2). The drift chamber system will be studied to find a way to operate with better single electron efficiency in 1999. Also, the most

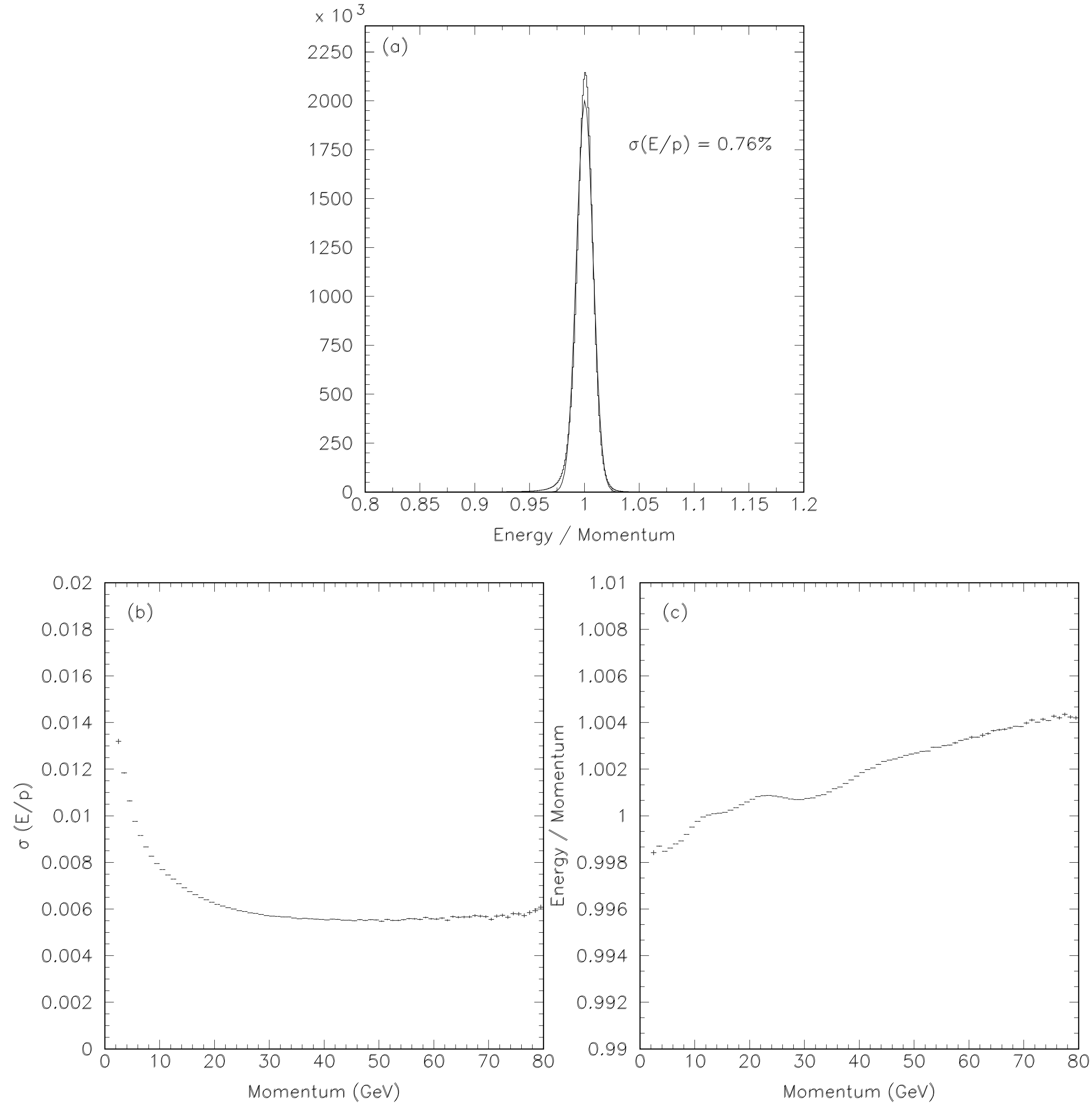

Figure 2: (a) Measured E/p (calorimeter energy / spectrometer momentum) for a sample of electrons from $K_L \to \pi^+ e^- \nu$ events; (b) σ(E/p) versus momentum for these electrons; (c) Measured E/p versus momentum for these electrons.

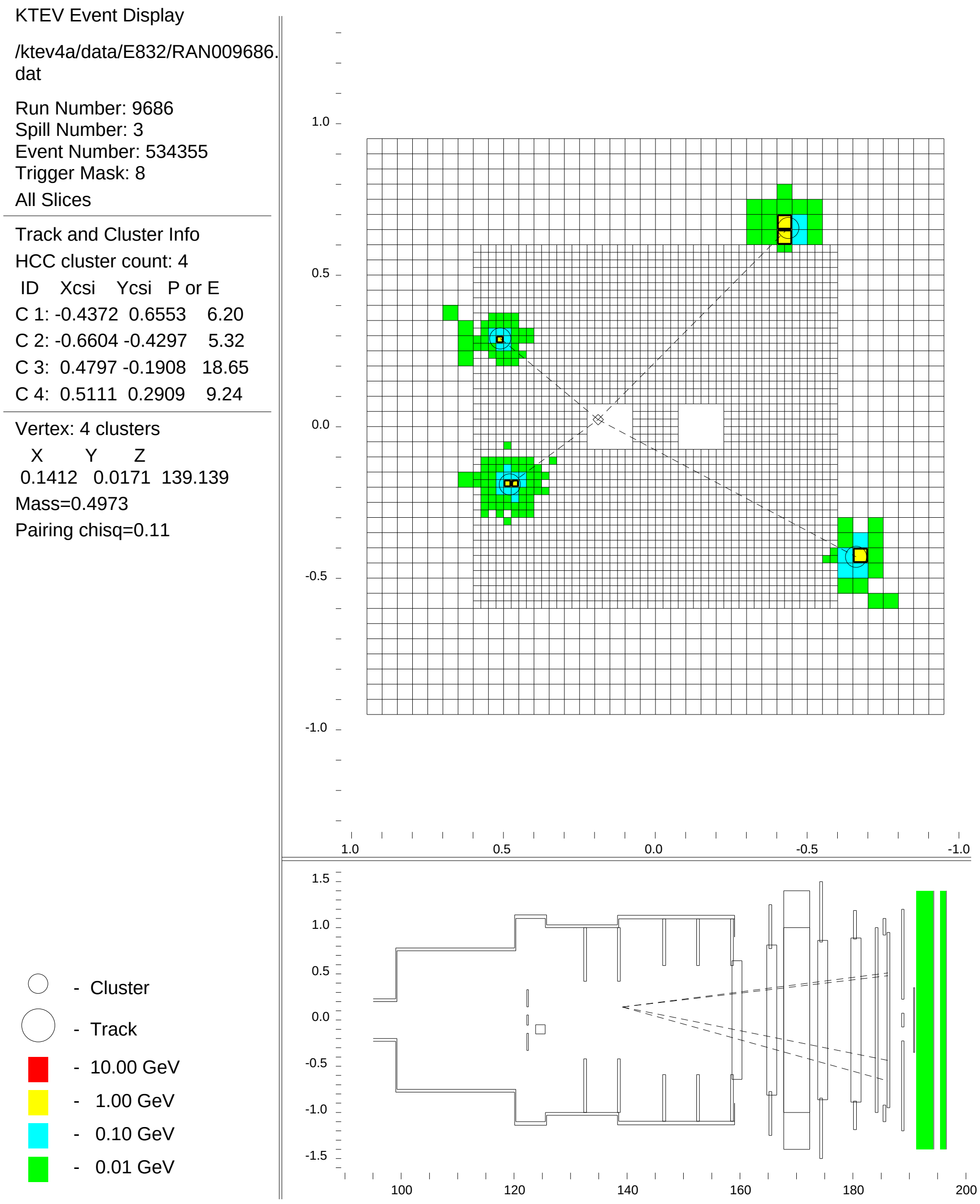

Figure 3: A typical online event display of a $K \to 2\pi^0$ decay.

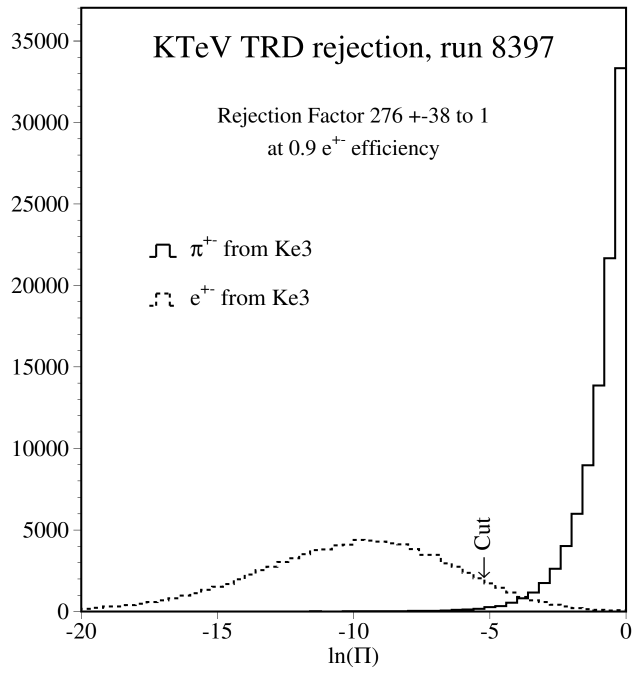

Figure 4: The log-likelihood function used for π/e rejection by the TRD system.

upstream drift chamber sustained substantial radiation damage in the beam region. This part of the chamber will be restrung for the 1999 run.

3. Livetime. The level 2 decision time and the detector readout time were longer than expected. Although these times were partially offset by lower than expected trigger rates, we plan to reduce the trigger decision time and readout time for the 1999 run.

2.2 E832 - ϵ'/ϵ Measurement

The primary goal of the KTeV experiment is to measure the direct CP violation parameter ϵ'/ϵ to a precision of 10^{-4}. This goal represents a factor of six improvement compared to the E731 result[2]: $\mathrm{Re}(\epsilon'/\epsilon) = (7.4 \pm 5.2 \pm 2.9) \times 10^{-4}$.

During the 1996-1997 KTeV run, we collected a data sample that includes 4 million $K_L \to \pi^0\pi^0$ events after preliminary offline cuts. About 1/4 of these data were collected during the fall of 1996 and the remaining 3/4 during the spring and summer of 1997 (see Table 1). This data sample should result in a statistical uncertainty of around 1.5×10^{-4} on ϵ'/ϵ. We hope to reduce the systematic error to about half of the statistical error, though achieving this goal may require a few years of effort.

Online invariant-mass plots for the 2-pion decay modes from the entire E832 data sample are shown in Fig. 5. The invariant-mass resolution of the online reconstruction is better than the best offline results from the previous round of experiments. The offline analysis will reject

$\sim 30\%$ of the signal events shown in these plots, while reducing the background level by an order of magnitude.

The offline analysis of the data is in progress. The first step in this analysis is to "split" the raw data tapes, which contain a mix of all types of events, into tapes containing different classes of events. This split has been completed for the 1996 data sample, and will be completed by February 1998 for the 1997 data. The offline calibration of all detector elements is nearly complete for the 1996 data and is beginning for the 1997 data. This calibration includes alignment of all detectors, energy calibration of photon veto detectors, time-to-distance calibration of drift chambers, and energy calibration of the CsI calorimeter. We are beginning detailed comparisons of data and Monte Carlo to evaluate the detector acceptance.

Significant effort has gone into studying systematic biases in the charged spectrometer. Following the 1996 run, we discovered that we had been operating with a significantly lower efficiency for single drift electrons in the drift chambers than in past experiments (i.e., the electronic threshold was higher relative to the avalanche pulse from a single drift electron).[2] This lower efficiency, combined with online tracking code that was based on E731 offline chamber performance, led to a 20% loss of charged-mode data during the 1996 ϵ'/ϵ run. Offline studies have shown that the loss of events was slightly different in the regenerator and vacuum beams, and if not corrected, would result in a significant bias in ϵ'/ϵ. After several months of work, we have not yet found a way to correct the 1996 data without greatly increasing the uncertainty in the result. For the 1997 run, the online tracking requirements were relaxed to reduce the sensitivity to the exact value of the threshold. If we are unable to use the charged-mode data from 1996, the precision of the final result (i.e., 1996 + 1997) will not be compromised; even without the the 96 charged-mode data, most of the statistical error will come from the neutral mode.

Besides the ϵ'/ϵ measurement, the current E832 data will result in significantly improved measurements of the the regeneration phase, Δm, $\Delta\phi$, ϕ_{+-}, $K_L \to \pi^+\pi^-\gamma$, $K_L \to \pi^0\gamma\gamma$, the K_{e3} charge asymmetry, as well as some rare K_S decay searches.

2.3 E799-II - Rare Kaon Decays

During 1997, part of the KTeV running time was devoted to the rare kaon decay experiment, E799-II. The E799 detector configuration differed from that used for E832 in several important respects: the regenerator was moved out of the beams, resulting in two parallel K_L beams; the transition radiation detectors, which were not used in E832, were moved into position between the last drift chamber and the trigger scintillator banks; the most upstream photon veto detector was removed to increase the acceptance; and finally, the beam size and intensity were increased to improve the rare decay sensitivity.

E799 used a wide variety of triggers, each designed to be sensitive to a particular set of interesting rare decays. Among the most important were the "two-electron+N-cluster" trigger, which was designed with $K_L \to \pi^0 e^+e^-$ decays in mind; the di-muon trigger, which selected $K_L \to \pi^0\mu^+\mu^-$ events and other events with two muons in the final state; and the Dalitz trigger, designed for $K_L \to \pi^0\nu\bar{\nu}(\pi^0 \to e^+e^-\gamma)$.

[2] We would have liked to have higher gain in the chamber system. Unfortunately, the high voltage could not be increased without drawing excessive current at the proton intensity we wanted to use, and the electronic gain could not be increased without too high a rate of spurious hits from noise.

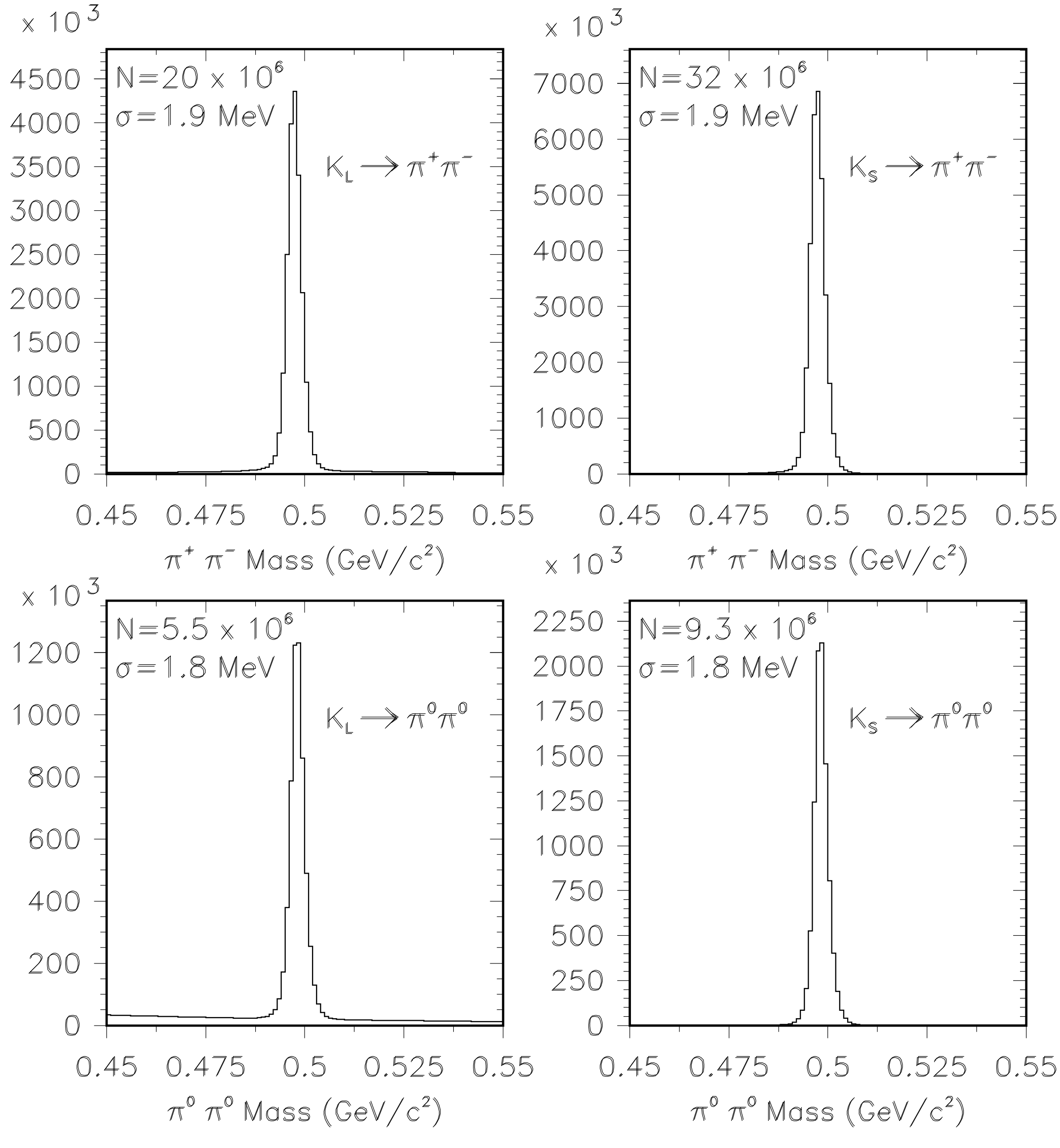

Figure 5: Online invariant-mass plots from the entire E832 run for $K \rightarrow \pi^+\pi^-$ (top) and $K \rightarrow \pi^0\pi^0$ (bottom) for vacuum (left) and regenerator (right) beams.

E799 data were collected from mid-January until late March 1997, and again for about four weeks at the end of the run in August. Taking accelerator down time in account, this amounted to about eleven weeks of running. The detector performed well, but still suffered about 25% down time due to the problems mentioned in Section 2.1, above. The net result was an E799 data set of about 50 "good-days" of data, from which over one billion events were selected by the online filter programs and written to tape for later analysis.

The performance of E799 was monitored online, and the sensitivity of the experiment was gauged by recording the number of so-called "three-π^0-Dalitz" events reconstructed online from the two-electron+N-cluster trigger. These events were $K_L \to \pi^0\pi^0\pi^0$ decays in which two of the π^0's decayed to two photons, and the third decayed to $e^+e^-\gamma$. The overall probability of a K_L decaying this way is about 0.76%. During the E799 running, over ten million of these events were reconstructed using loose level 3 cuts.

The level 3 software also performed online reconstruction of several moderately rare K_L decays, such as $K_L \to e^+e^-\gamma$ and $K_L \to \mu^+\mu^-\gamma$. The branching ratios for these modes are about 9×10^{-6} and 3×10^{-7}, respectively. The more common $e^+e^-\gamma$ mode showed an online mass peak within just a few minutes of running, while the rarer muonic Dalitz decay showed a clear mass peak within a few hours. During the whole 1997 run, several thousand examples of $K_L \to \mu^+\mu^-\gamma$ were identified. This is particularly remarkable in view of the fact that only a single event of this type had been identified prior to the E799-I branching ratio measurement based on 207 events, published in 1995. Figure 6 shows the yields of these electronic and muonic Dalitz decays for one-day of data from the 1997 run.

Further analysis began with the selection of a few runs from a single good day of running. These runs represented about 2% of the full E799-II data set. The initial calibration efforts focussed on this small data set so that analysis programs could be exercised, and code tuned-up, in anticipation of the full analysis to begin later.

Though this "one-day" data set was originally viewed as a tool for testing reconstruction and analysis procedures within the collaboration, it soon became clear that there were important new physics results even in this small data sample. For example, these data revealed the first unambiguous signal for the rare decay $K_L \to \pi^+\pi^-e^+e^-$. After all cuts, several dozen events were identified in the one-day data sample, and a preliminary branching ratio of $(2.6 \pm 0.5) \times 10^{-7}$ was determined for this mode. A Letter reporting this result is currently being prepared for submission to the Physical Review. The $\pi^+\pi^-e^+e^+$ mode is particularly intriguing because it is expected to exhibit a large CP-violating asymmetry in the angular distribution of the final-state particles[9]. A preliminary, "express-line" analysis of about half of the E799-II Winter data set already shows strong evidence for an asymmetry similar to the one predicted, based on a sample of a few hundred events. Details of this analysis are described in Section 2.4.

The one-day data sample has also been used to make more detailed acceptance and detector performance studies. Consistent with the yield found by the online software, over 200k three-π^0-Dalitz events have been reconstructed in the one-day data. This relatively high-statistics sample has been used to study tracking and clustering performance, apertures, and other details in preparation for the analysis of the full E799-II data set.

The event yields from the one-day data allow us to determine the total number of kaon decays to which the detector was exposed during that day. Based on the number of events reconstructed in several of different modes, and from a number of different triggers, we find

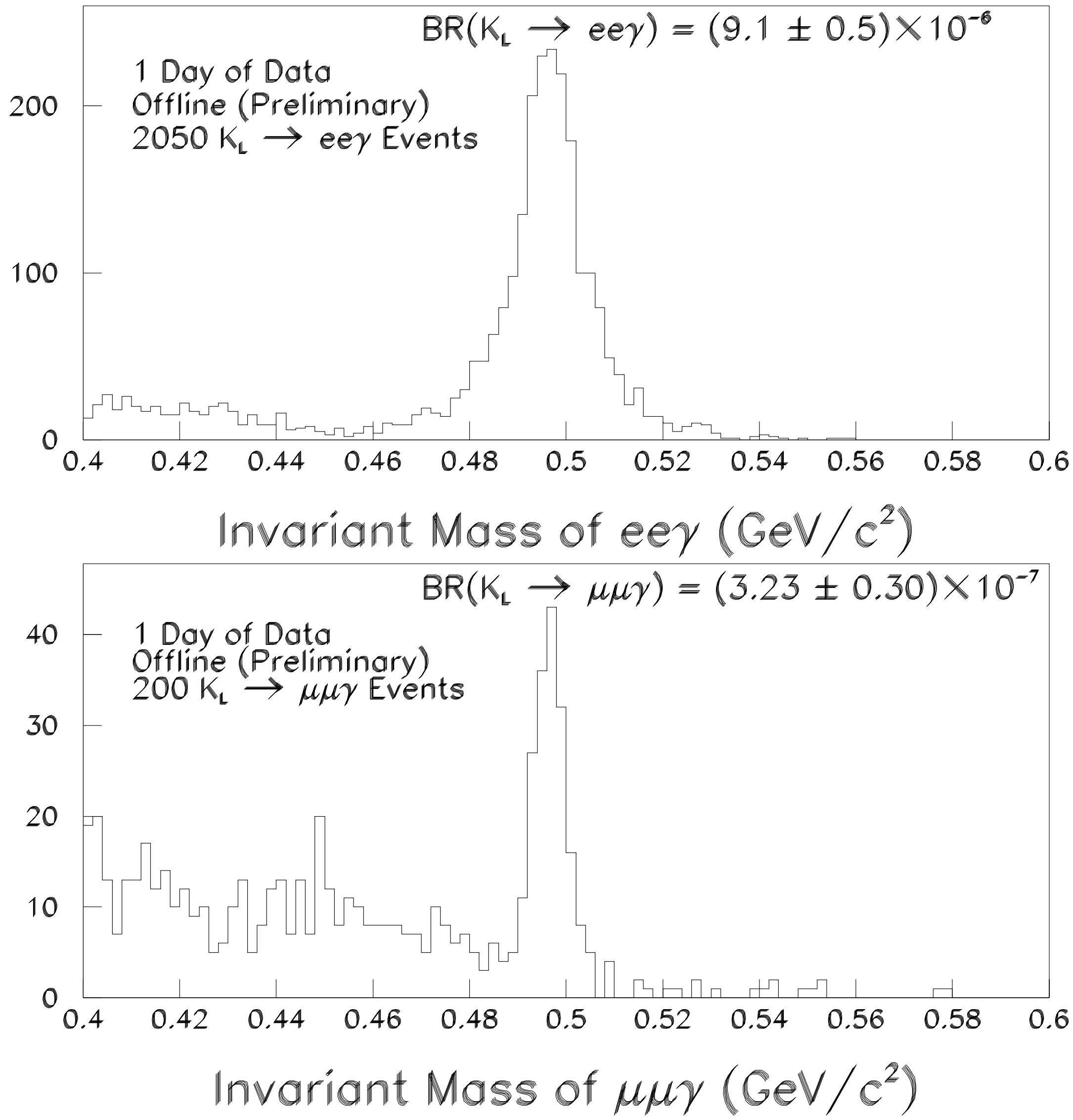

Figure 6: K_L Dalitz decay yields from the one-day analysis.

a flux of $(4.9 \pm 0.2) \times 10^9$ K_L decays for the one-day data. Since this is only 1/50 of the full 1997 data set, we estimate the flux for all the 1997 running at about 2.5×10^{11} K_L decays. Based on an acceptance estimate of 5%, this should correspond to a single-event sensitivity (SES) for $K_L \to \pi^0 e^+ e^-$ of about 8×10^{-11}. Similar estimates have been made for the other $K_L \to \pi^0 l \bar{l}$ modes; the results are summarized in the table below.

Mode	Projected SES
$K_L \to \pi^0 e^+ e^-$	8×10^{-11}
$K_L \to \pi^0 \mu^+ \mu^-$	1×10^{-10}
$K_L \to \pi^0 \nu \overline{\nu}$ $(\pi^0 \to e^+ e^- \gamma)$	1×10^{-7}

Table 3: Projected sensitivities for CP violating decays from E799 run in 1997

It must be emphasized that the final E799-II limits on each of these modes is likely to be background-limited, so that the 90% confidence-level upper limits on the branching ratios will not simply be 2.3 times the single-event sensitivity. For example, E799-I has already measured the radiative-Dalitz decay $K_L \to e^+ e^- \gamma\gamma$. This decay can mimic the $\pi^0 e^+ e^-$ mode, and will undoubtedly provide background in the $\pi^0 e^+ e^-$ search region[10]. The exact level of this background will not be known for some time, and it can be reduced by making full use of the excellent energy resolution of the CsI calorimeter. But even with this background, E799-II should be able to reduce the 4.3×10^{-9} 90% confidence level upper limit[11] on the branching fraction for this mode by approximately an order of magnitude.

The combination of improved acceptance, increased beam intensity, and reduced dead-time allowed E799-II to match the sensitivity of E799-I within two good days of running, and should result in its surpassing the sensitivity of E799-I by a factor 25 for most modes, and by even greater factors in the case of some modes, such as $K_L \to e^+ e^- \gamma$ and $K_L \to \pi^+ \pi^- e^+ e^-$, the triggers which had to be prescaled in the E799-I run.

As with E832, the first step in the full analysis is to separate the various triggers into different data sets via a software split. Because there were so many triggers in E799, there are over a dozen split output streams. Some of these contain data from more than one trigger. The split of all E799 data was completed on December 1, 1997.

The next stage in the analysis of the data will be to run filter programs on the split output tapes to make smaller sets of DSTs tailored to particular physics analyses. Such a program is already being run on the four-track trigger data so that we can extend our study of the $K_L \to \pi^+ \pi^- e^+ e^-$ mode using the full E799-II data set as soon as possible. A "crunch" of the two-electron+N-cluster data is also planned to begin in December 1997. Physics results based on the full E799-II statistics should begin to appear during 1998.

2.4 Preliminary Rare Kaon Decay Physics Results

Even though the analysis of the 1997 E799-II data is still at a very early stage, we can already report progress on a number of fronts. In this section we give a more detailed review of two of these preliminary rare decay results. The first is the search for, and first observation of, the decay $K_L \to \pi^+\pi^-e^+e^-$. This decay, although not one of the places where direct CP-violation is expected to be a big effect, nevertheless exhibits a unique window for the study of indirect CP-violation. The second analysis described here, the search for $K_L \to \pi^0\nu\bar{\nu}$ using a special one-day run in 1996, concerns what is doubtless the most theoretically attractive of the rare kaon decays. The method of analysis and some of the potential difficulties due to backgrounds will be discussed.

2.4.1 $K_L \to \pi^+\pi^-e^+e^-$

The rare decay $K_L \to \pi^+\pi^-e^+e^-$ has been unambiguously observed[12] for the first time in the 1997 KTeV run. A special four-track trigger was designed to collect these events. Most of the events which fire this trigger come from the relatively common $K_L \to \pi^+\pi^-\pi^0$ decay, followed by a Dalitz decay $\pi^0 \to e^+e^-\gamma$. These events are in fact quite similar to the $\pi^+\pi^-e^+e^-$ signal, and are used to normalize the flux in this analysis. To separate the signal from the background due to this process, a cut is made on $p_\perp^2$, the transverse momentum of the observed four charged particles with respect to the kaon line-of-flight (the line connecting the target to the decay vertex). To reduce the background further, we calculate a quantity $P_{\pi 0}^2$ which is equal to the square of the longitudinal momentum of the π^0 for the background hypothesis $K_L \to \pi^+\pi^-\pi^0$. This quantity depends only on the measured momentum of the charged pions, and should be positive definite for real $K_L \to \pi^+\pi^-\pi^0$ decays, aside from resolution effects. About 90% of $K_L \to \pi^+\pi^-e^+e^-$ events have a negative value for $P_{\pi 0}^2$, so this cut very effectively separates the signal from the background.

In the E799-II one-day data sample, there is a clear signal of about 35 events after making the above cuts. Based on this sample, we have reported a preliminary branching ratio of $(2.6 \pm 0.5) \times 10^{-7}$. In view of this interesting finding, a preliminary analysis has been performed on a larger data set, representing about three weeks of E799-II running. The results are shown in Fig. 7. After all cuts, the mass peak from this data set includes about 460 events over a background estimated at 88 events.

The $K_L \to \pi^+\pi^-e^+e^-$ decay mode involves four distinct final-state particles, and therefore possesses a rich structure of final-state kinematic and angular distributions. It is expected to proceed dominantly through a $\pi^+\pi^-\gamma^*$ intermediate state. Two amplitudes of comparable size are expected to dominate the process. The first describes the CP-violating decay $K_L \to \pi^+\pi^-$ combined with internal bremsstrahlung of a virtual photon from the charged pions. The second corresponds to the M1-direct emission of a virtual photon, and is CP-conserving. The interference of these amplitudes results in a CP-violating photon polarization. While this polarization cannot be observed in the $\pi^+\pi^-\gamma$ final state, it reveals itself through the angular distributions of the final-state particles when the photon is virtual and converts to an e^+e^- pair. Specifically, the distribution of the angle ϕ between the $\pi\pi$ and ee decay planes is predicted to contain a CP-violating term proportional to $\sin 2\phi$. Unlike other CP-violating effects previously observed, this effect is predicted to be quite large, and

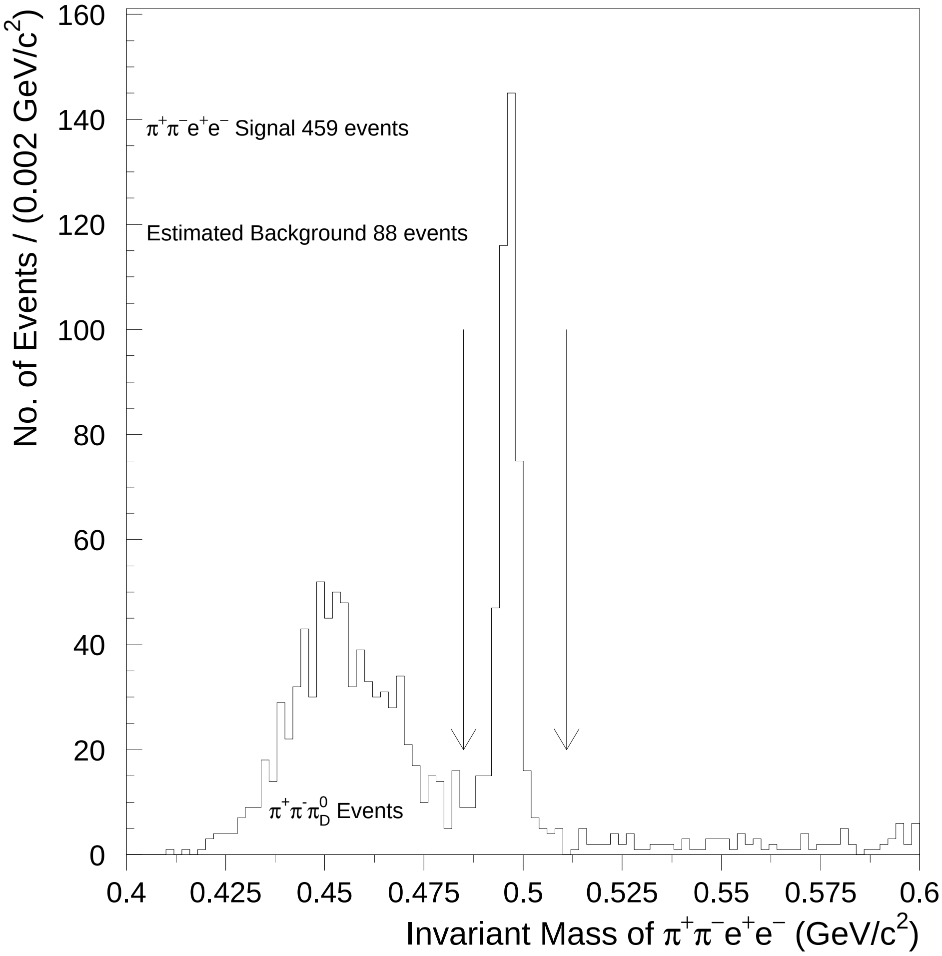

Figure 7: $K_L \to \pi^+\pi^-e^+e^-$ mass peak from the three-week data set.

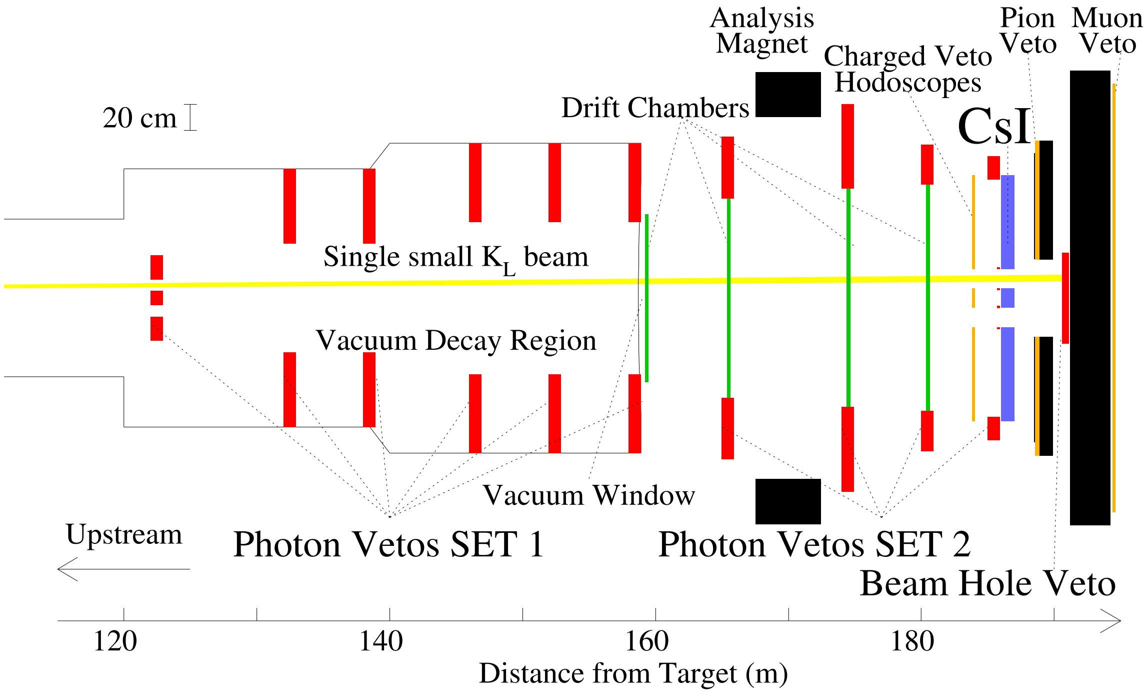

Figure 8: Schematic of the KTeV detector configuration used in the special $\pi^0\nu\overline{\nu}$ run.

should be easily observable even with a sample of just a few hundred events.

It is interesting to note that this effect, if observed, would be only the fourth manifestation of CP violation detected, the first three being the original discovery of K_L decays to two pions, the semileptonic charge asymmetry in K_{e3} and $K_{\mu 3}$ decays, and, most recently, the interference between K_S and K_L decays to $\pi^+\pi^-\gamma$ observed by E731 and E773 at FNAL[13]. KTeV should ultimately provide the best measurement of each of these effects.

2.4.2 $K_L \to \pi^0\nu\overline{\nu}$

The best limit on $K_L \to \pi^0\nu\overline{\nu}$ from E799 will ultimately come from using the Dalitz decay of the π^0. However, in order to eventually reach Standard-Model sensitivity levels, it will be necessary to use the eighty-times more common neutral decay $\pi^0 \to \gamma\gamma$.

A special half-day run at the end of 1996 was devoted to a test to see whether the neutral analysis could be successful in the future. During this special run, a single small beam (4×4 cm^2 at the CsI) was used in order to obtain good $p_\perp$ resolution. The second beam was completely closed off. Figure 8 shows a schematic of the detector configuration used for this special run.

The trigger was designed to detect $K_L \to \pi^0\nu\overline{\nu}$ as well as $K_L \to \pi^0\pi^0$ decays. The latter decay mode was used for normalization. At the trigger level, the CsI calorimeter was required to have two clusters of energy, with a total energy of at least 5 GeV. The events were required to have no activity in the trigger hodoscopes in order to reject events containing charged tracks. All photon veto detectors were required to have in-time energy deposits of less than

500 MeV.

The two missing neutrinos and the lack of any charged information make the analysis difficult because there are only two handles available to separate signal from background:

1. The z vertex determined from the two photon clusters, assuming the π^0 mass, which must reconstruct within the fiducial volume of the detector; and
2. The transverse momentum, $p_\perp$ of the reconstructed π^0, with respect to the beam direction. The maximum possible $p_\perp$ from $K_L \rightarrow \pi^0\nu\overline{\nu}$ decays is 231 MeV/c. A small kaon beam is necessary in order to obtain good $p_\perp$ resolution since the assumption is made that the decay originated at the transverse center of the beam.

The Z position of the decay vertex for $\pi^0\nu\overline{\nu}$ candidates was determined by constraining the two clusters in the calorimeter to reconstruct to the π^0 mass. The resolution of the Z vertex obtained by this method is approximately 30 cm. Figure 9 shows the $p_\perp$ distribution for these events as a function of the Z position of the decay vertex. π^0 production due to hadronic interactions in the vacuum window can be clearly seen as a vertical band near $Z = 160$ m. The band of events near $p_\perp = 100$ MeV/c is from the decays $\Lambda \rightarrow n\pi^0$. The vertical band around $Z = 122$ m is due to interactions of the beam halo with the most upstream photon veto detector. The chosen decay region for the signal search was $125 < Z < 157$ m, as indicated by the box in the figure. A similar plot from a Monte Carlo simulation of $\pi^0\nu\overline{\nu}$ decays is also shown in Figure 9.

More stringent selection criteria were applied in the offline analysis. Events with additional clusters in the calorimeter which had a deposited energy of greater than 100 MeV were discarded. The transverse profile of the two reconstructed energy clusters was required to be consistent with that of a single electromagnetic shower, reducing background from fusions, in which two or more photons overlap to give rise to a single cluster. Events with hits in the drift chamber system were also eliminated.

Events in which the energy deposited in the set-1 photon veto detectors (see Figure 8) was greater than 70 MeV were rejected. In addition, the energy deposited in the set-2 photon veto detectors (Figure 8) was required to be less than 5 MeV to help reduce the background from beam neutron interactions in the detector. The beam hole veto detector was required to have an energy deposit of less than 400 MeV. To reduce the Λ background, the total energy deposited in the calorimeter was required to be less than 35 GeV. Most of the Λs which survive until the beginning of the decay region of the detector are of very high energy, averaging approximately 200 GeV.

Figure 9 shows the $p_\perp$ vs. Z distribution for our data sample after final cuts. The signal search region is enclosed by the box. The $p_\perp$ distribution of the events in the decay region $125 < Z < 157$ m is shown in Figure 10. The signal search region is defined as $160 < p_\perp < 260$ MeV/c. The observed $P_\perp$ distribution is well reproduced by a $K_L \rightarrow \gamma\gamma$ and a $\Lambda \rightarrow n\pi^0$ Monte Carlo. One event remains in the signal search region.

A clean signal is observed in the normalization mode $K_L \rightarrow 2\pi^0$, as shown in Figure 11. There are 4326 events in the peak with an estimated background of 44 events. The Monte Carlo acceptances for the decays $K_L \rightarrow \pi^0\nu\overline{\nu}$ and $K_L \rightarrow 2\pi^0$ were found to be 3.6% and 6.7% respectively. This results in a single event sensitivity for the decay $K_L \rightarrow \pi^0\nu\overline{\nu}$ of 4.04×10^{-7}.

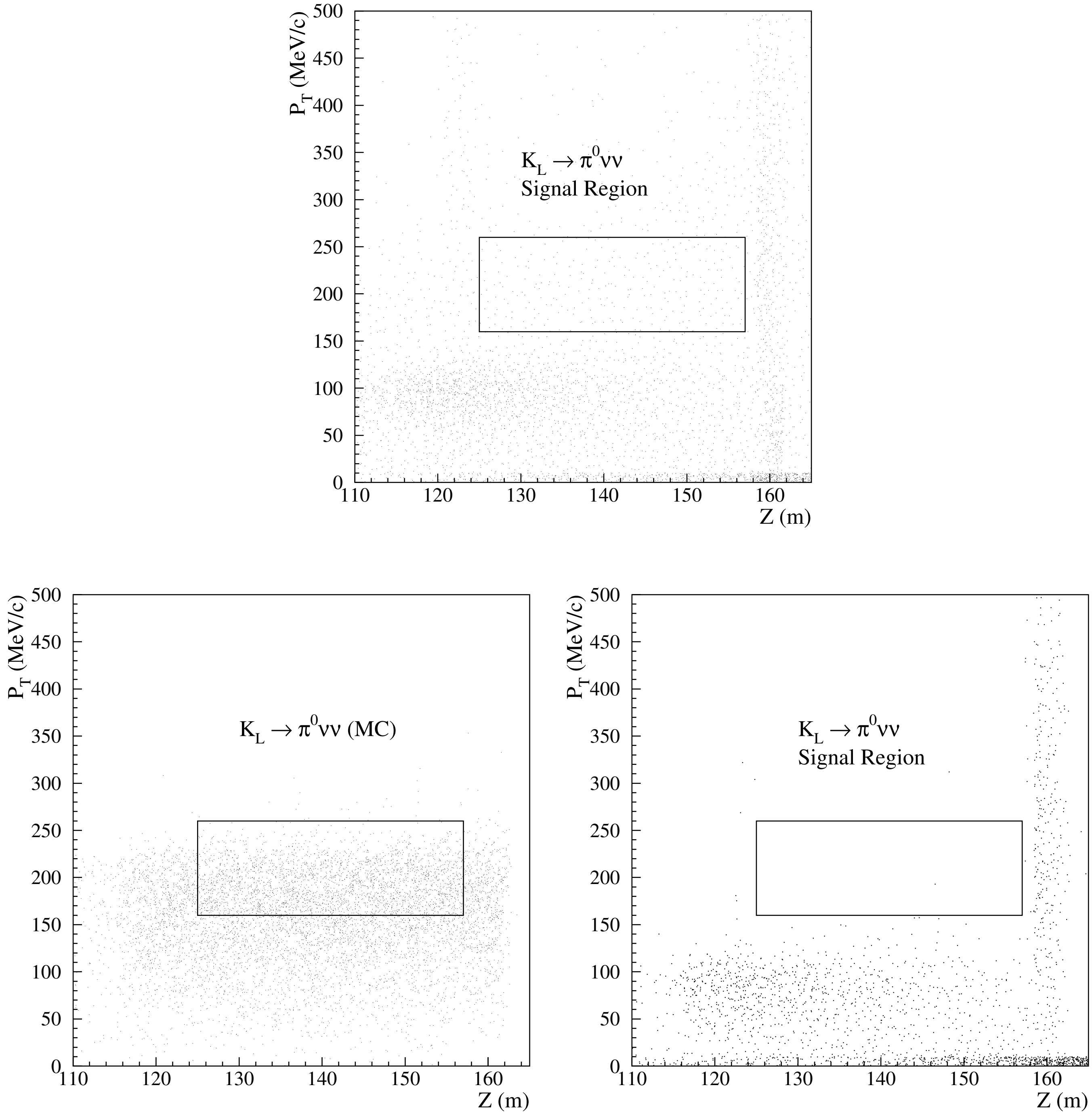

Figure 9: Scatter plots of $p_\perp$ vs. the Z decay vertex for $K_L \to \pi^0 \nu \overline{\nu}$ candidates. The top plot shows the distribution after trigger level cuts, the bottom left plot is from a Monte Carlo simulation of the signal and the bottom right plot is the data after the final selection cuts described in the text. In each case, the signal search region is indicated by the box.

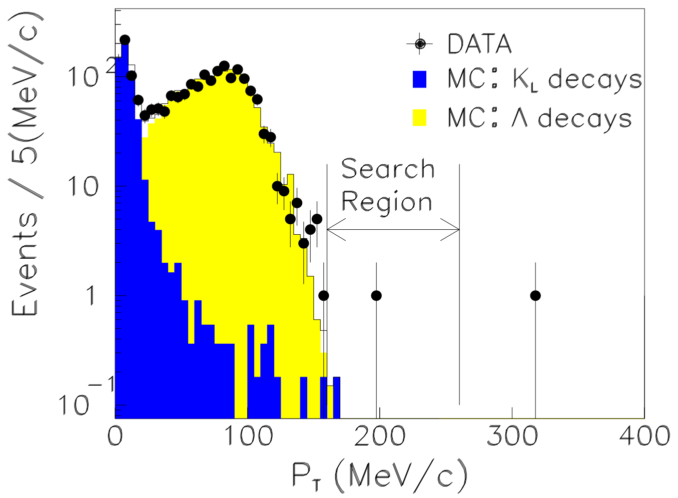

Figure 10: The $p_\perp$ distribution after final cuts of $K_L \to \pi^0 \nu \overline{\nu}$ candidate events using the 2γ decay mode of the π^0.

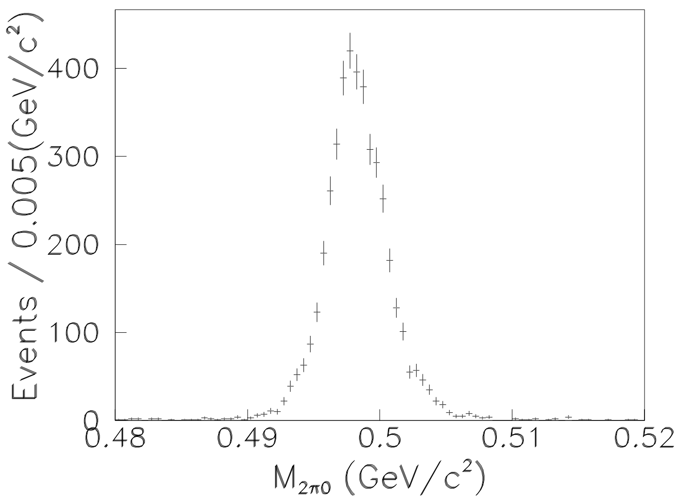

Figure 11: The $K_L \to 2\pi^0$ mass peak used for normalization in the $K_L \to \pi^0 \nu \overline{\nu}$ search.

The one remaining event in the signal search region was found to be consistent with beam neutron interactions. The background level from K_L, Λ, and Ξ^0 decays was found to be negligible (SES $\simeq 1 \times 10^{-9}$, see section 3.4.1 below).

To investigate the background resulting from neutron interactions, we removed the requirement of the beam hole veto, which resulted in 37 events remaining in the signal region. This sample of events has three components. The first component results from events in which a neutron is identified by activity in the downstream section of the beam hole veto. The second component comes from neutrons which interact in the upstream section of the beam hole veto. The last component is the result of photons in the event which are detected in the upstream section of the beam hole veto.

Using a sample of $\Lambda \to n\pi^0$ decays, we have determined that the neutron detection efficiency is 82% for neutrons incident on the beam hole veto. In the sample of 37 events, 31 (84%) produced activity in the downstream section of the detector, consistent with the measured 82% neutron efficiency. Of the 37 events, 26 had activity in the upstream section of the detector. These 26 events are a combination of events which contain photons and events in which an neutron interacts in the upstream section of the detector.

Using the $\Lambda \to n\pi^0$ events we have measured the neutron detection efficiency to be 44% in the upstream section of the beam hole veto. To determine the fraction of the 26 events in which a photon struck the beam hole veto and was detected, we used the following expression: $26/37 = (1-r)\times 0.44 + r$, where r is the fraction of events with a photon detected by the beam hole veto, and 0.44 is the neutron detection efficiency. From this expression we determined that r is 0.47 ± 0.25. Therefore, the number of background events which do not fire the beam hole veto is estimated to be $37\times(1-0.82)\times[1-(0.47\pm 0.25)] = 3.5\pm 1.7$ events. In this expression, 37 is the number of events before requiring the beam hole veto, $(1-0.82)$ is the neutron detection inefficiency, and $[1-(0.47\pm 0.25)]$ is the fraction of the events in which no photon is detected by the beam hole veto. Using the same method, we also estimate the number of background events in the $p_\perp$ region above the signal region to be 0.57 ± 0.27, consistent with one observed event. Therefore, we conclude that the one observed event in the signal region is consistent with background from a neutron interaction.

Based upon one observed event in the signal search region, we set a preliminary upper limit on the $\pi^0\nu\overline{\nu}$ branching ratio, $BR(K_L \to \pi^0\nu\overline{\nu}) < 1.6 \times 10^{-6}$ at the 90% CL[14]. This represents a factor of 30 improvement over the best existing limit, obtained by E799-I using the Dalitz decay mode of the π^0[15].

It is evident from this analysis that the limiting background for the $\pi^0\nu\overline{\nu}$ search with the KTeV detector in 1999 will be beam neutron interactions in the detector. In light of this result, it is clear that such hadronic interactions need to be vetoed effectively in order to achieve greater sensitivity in this search. We propose to build a new beam hole veto which will reduce our beam neutron inefficiency from 18% to 1% (see Section 4.7).

2.5 E799-II - Hyperon Decays: Status and Preliminary Results

Even though the KTeV experiment is situated relatively far from the production target (approximately 90 meters), a significant number of Λ and Ξ^0 hyperons survive to reach our decay volume. During the single day of E799 data discussed above, the Ξ^0 and Λ fluxes were 4.9×10^6 and 1.1×10^8 ($\pm$ 20%), respectively. Concurrent with the rare kaon data taking, we collected about 200 million hyperon decay triggers during the two E799-II running periods in 1997.

Between the two running periods we improved our trigger to enhance our sensitivity to the beta decay: $\Xi^0 \to \Sigma^+ e^- \overline{\nu}$, followed by $\Sigma^+ \to p\pi^0$. We have approximately 900 candidate events on tape.

The opportunity to investigate this decay is particularly intriguing for at least four reasons.

1. It had never been observed before E799-II.

2. It is the analogue of the well-measured neutron beta decay: $n \to pe^-\overline{\nu}$ under d and s quark interchange. Thus, in the flavor symmetric quark model, differences between these two decays arise *only* from the differing particle masses and from the relevant CKM mixing factors (V_{us} rather than V_{ud}). The predicted branching ratio is 2.61×10^{-4}. Theoretically interesting flavor symmetry violation[16] effects can be readily isolated if they occur in this decay.

3. The polarization of the final state Σ^+ can be readily measured. The primary decay: $\Sigma^+ \to p\pi^0$ has a proton asymmetry parameter of -0.98, thereby providing direct information about interference effects in the beta decay equivalent to that from a Ξ^0 sample with a 98% polarization!

4. There is no competing two-body decay with a Σ^+ in the final state. (The decay $\Xi^0 \to \Sigma^+\pi^-$ would violate energy conservation.) This eliminates a problematic source of background which is present in other hyperon beta decays.

The KTeV97 run provided the first observation of the Ξ^0 beta decay: $\Xi^0 \to \Sigma^+ e^- \overline{\nu}$ (with subsequent $\Sigma^+ \to p\pi^0$ decay). This distinctive signature, combined with the excellent resolution of the KTeV detector, provides a signal which is sufficiently clean that we are able to perform our initial analysis using online calibrations from the first E799 running period. We searched for double vertex events where there is a Σ^+ reconstructed from a proton and a π^0 (π^0 mass constrained) downstream of the vertex formed by an electron track and the 'track' from the reconstructed Σ^+. Electrons were identified with the CsI calorimeter. Figure 12 shows the reconstructed Σ^+ mass peak with a Monte Carlo overlay. Using a subsample of events collected with stable detector operating conditions, and normalizing to a reference sample of $\Xi^0 \to \Lambda\pi^0$ decays which was collected simultaneously, we obtain a branching ratio of $(2.4 \pm 0.2 \text{ (stat)} \pm 0.3 \text{ (syst)}) \times 10^{-4}$. A paper presenting this result is in preparation. When the full data sample is available along with refined offline calibrations, decay asymmetries will be determined as well as a more precise branching ratio.

A second process amenable to study with online calibrations is the weak radiative decay $\Xi^0 \to \Sigma^0\gamma$. Theoretical predictions for the branching ratio and asymmetry parameter vary widely. There is only one experiment[34] in the literature with a sample of 85 events. Since $c\tau$ for the Σ^0 is very small (it decays electromagnetically), both photons effectively come from the same vertex. The topology is therefore the same as $\Xi^0 \to \Lambda\pi^0$, the dominant decay mode. We reconstruct the radiative decay by assuming a Ξ^0 mass. Given the reconstructed Λ 'track', it is then possible to reconstruct a vertex. Events in which the two photons have an

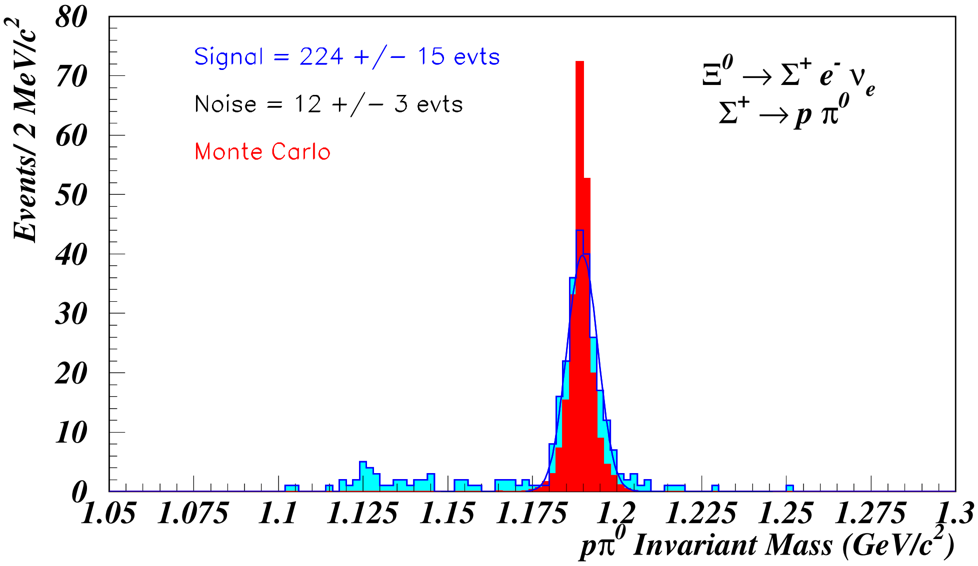

Figure 12: Evidence for the first observation of $\Xi^0 \to \Sigma^+ e^- \overline{\nu}$, with $\Sigma^+ \to p\pi^0$. The reconstructed Σ^+ mass is plotted along with a Monte Carlo overlay (dark region).

invariant mass consistent with the π^0 mass are removed from the sample. The $\Lambda\gamma$ invariant mass is then formed with each of the two photons, and the combination closest to the Σ^0 mass is selected. The resulting $\Lambda\gamma$ mass spectrum for data from the first E799-II running period is shown in Figure 13. Data from the full KTeV97 run contains about 50 times more events than the present world sample.

We also recorded a sample of the weak radiative decay $\Xi^0 \to \Lambda\gamma$ which is about 7 times larger than that in the previous experiment[35]. Here too a self-analyzing final state hyperon provides information on sought-after[17] parity violating interference effects (asymmetry parameters).

Additional analysis efforts are under way to observe the muonic beta decay $\Xi^0 \to \Sigma^+ \mu^- \overline{\nu}$, to study $\overline{\Xi^0}$ decays, and to search for the $\Delta S = 2$ second-order weak decay $\Xi^0 \to p\pi^-$. We also plan to use our reference sample of 300,000 $\Xi^0 \to \Lambda\pi^0$ decays to reduce the Ξ^0 mass uncertainty (now $\pm$ 0.6 MeV/c^2) which currently limits the precision with which the Coleman-Glashow mass relation can be tested[18].

2.6 Results of R^0 search

A search for a light gluino, called the R^0, through its dominant decay mode $R^0 \to \tilde{\gamma}\rho$ with $\rho \to \pi^+\pi^-$, has been performed on a one-day E832 data sample. This search is motivated by recent predictions in the literature[19][20]. The photino in this SUSY scenario is a cold dark matter candidate, which suggests a range of 1.3 - 2.2 GeV/c^2 for the R^0 mass and a range of 0.1 - 100 ns for the R^0 lifetime. This is the first time a direct search for such a decay has been performed. Figure 14 shows the $\pi^+\pi^-$ invariant mass distribution for the data (solid)

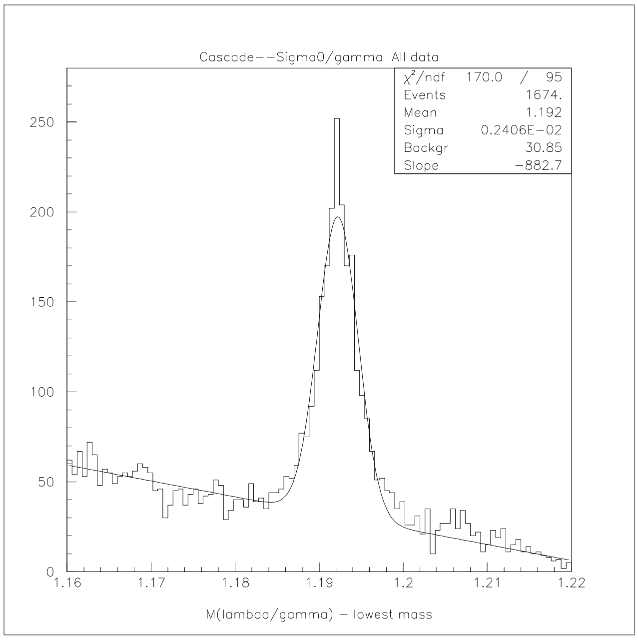

Figure 13: Evidence for the cascade radiative decay $\Xi^0 \rightarrow \Sigma^0\gamma$ with $\Sigma^0 \rightarrow \Lambda\gamma$. The $\Lambda\gamma$ mass spectrum is plotted.

and an R^0 Monte Carlo (dashed). The R^0 search region is above the $\pi^+\pi^-$ invariant mass of 648 MeV/c^2. Using one day of data, we are sensitive to R^0 decays in the mass and lifetime ranges of 1.2 to 4.6 GeV/c^2 and 2×10^{-10} to 7×10^{-4} s, respectively. The upper limit on the invariant cross section $Ed^3\sigma/dp^3$ times the branching ratio for the R^0 is in the range of $1 \times 10^{-35}\mathrm{cm}^2/(\mathrm{GeV}^2/\mathrm{c}^3)$ at $x_F = 0.2$. These results were recently published[21].

3 Continuation of the Ongoing Program in 1999

A significant run in 1999 will be an important step in the continuing neutral kaon program at Fermilab. The kaon flux from the combined FY97 and FY99 runs will allow us to complete our measurement of ϵ'/ϵ and to reach our proposed sensitivities for a wide array of decay modes. It can also play a significant role in helping us plan for a future neutral kaon experiment at the Main Injector, KAMI (Kaons At the Main Injector)[22][23]. With upgrades over time and the availability of significantly larger kaon fluxes during the Main Injector era, it should eventually be possible to detect and measure $K_L \rightarrow \pi^0\nu\overline{\nu}$ as well as other important rare decay modes.

3.1 ϵ'/ϵ Measurement

The proposed new slow-spill length in 1999, with a 40 sec. flat top (increased from 20 sec.) and an 80 sec. spill cycle time (currently 60 sec.), will give us a 50% increase in kaon yield per hour without increasing the instantaneous rate in the detector at a nominal intensity of 7-8E12 protons per spill. An extrapolation from the current E832 run shows that we can

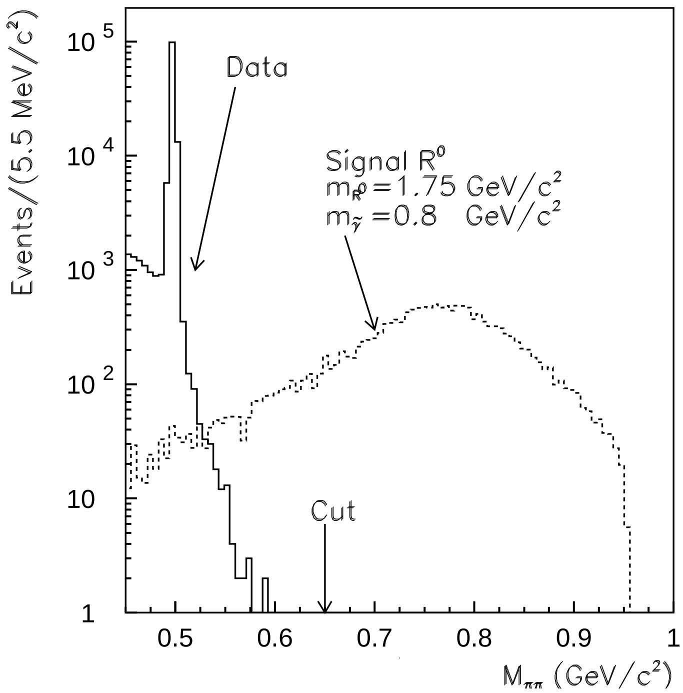

Figure 14: $\pi^+\pi^-$ invariant mass distribution used in the R^0 search.

collect an additional 4.5 million $K_L \to 2\pi^0$ decays in 10 weeks of running in 1999, doubling our current data sample. It is likely that the 1999 data will have much better systematic properties than the KTeV97 data sample. The combined 1996-1997-1999 data sample will include more than 8 million $K_L \to 2\pi^0$ decays, resulting in a statistical error on ϵ'/ϵ of 1×10^{-4}.

The improvement factors for the 1999 run relative to the 1996-1997 run are shown in Table 4. We've assumed that data can be collected at a slightly higher beam intensity than in 1997; high intensity running in our current data will be studied to verify that high quality data can be collected at this higher intensity. The DAQ livetime improvements are discussed in Section 4.5; the 10% improvement quoted in that section has been reduced to 5% because of the increase in proton intensity. The expected improvements in KTeV's data-taking efficiency are described in Section 4. The run time quoted for KTeV97 is the sum of 12.5 weeks from 1997 and 4.5 weeks from 1996.[3]

As described in Section 2.2, we are now making detailed studies of systematic limitations in our current data. If we find systematic problems in the data, such as the 1996 charged-mode problem, the additional 1999 ϵ'/ϵ run will allow us to address these problems and reduce the systematic uncertainty in the final result. The current data will also be studied to see if we can run with different absorber configurations to increase the relative fraction of vacuum decays we collect, thereby reducing the statistical error for an equivalent run period.

[3]KTeV and Tevatron efficiency improvements allowed us to collect data more quickly in 1997 than in 1996. To account for this change, we have reduced the effective 1996 run time from 7 to 4.5 weeks to match the average yield per week during the 1997 run.

	KTeV97†	KTeV99	Improvement
Proton Intensity	3.5E12	8E12	2.28
Repetition Cycle	60 sec.	80 sec.	0.75
Beam Size	9.3 x 9.3 cm^2	9.3 x 9.3 cm^2	1.00
Beam Absorber	In	In	1.00
Detector Efficiency	0.83	0.91	1.1
DAQ Livetime	0.7	0.73	1.05
Run Time	17 weeks	10 weeks	0.59
Improvement (KTeV99/KTeV97)			1.16

†Includes data from 1996 and 1997 E832 runs.

Table 4: Factors of improvement from KTeV97 to KTeV99 for E832

Ongoing studies show that some component of our drift chamber problems is related to the intensity in the vacuum beam, suggesting that it may be impossible to increase the vacuum beam intensity without compromising data quality.

3.2 Rare Kaon Decays

A second data-taking period in 1999 will allow substantial improvements in the rare decay sensitivity of E799-II. We are requesting a nine-week run, compared to about 11 weeks in 1997 (corrected to account for changes in the beam size between the winter and summer running). In spite of the shorter running time, we expect to be able to collect more than double the 1997 data, and to better than double the rare decay sensitivity.

This will be accomplished partly by taking advantage of the new slow spill duty cycle, which will provide a factor of 1.5 improvement in the kaon flux. In addition, we will make the beam size 40% larger than used for the Winter data set, gaining another factor 1.4. Finally, the improvements we are making to the level 2 trigger and data acquisition systems should together result in an increase from 70% to 73% in livetime, assuming a similar mix of triggers to that used in the 1997 E799-II run. The effect of combining these factors is shown in Table 5.

The improvement factor in the table will be achieved only if we have nine weeks of continuous good running conditions from the accelerator, as well as smooth detector performance. We would strongly prefer a longer run, which provides a safety factor in the event of down time. If we were fortunate enough to have 14 weeks of good running conditions, we could improve the overall sensitivities and rare decay statistics by a factor of four or more compared to the 1997 data alone.

Nevertheless, even assuming only nine weeks of running for E799-II in 1999, the potential increases in sensitivity, shown in Table 6, are substantial. We are convinced that these improvements, taken as a whole, more than justify the effort and cost of running E799-II in 1999.

In the case of $K_L \to \pi^0 e^+ e^-$, and $K_L \to \pi^0 \mu^+ \mu^-$, the addition of a 1999 run will allow our single-event sensitivity to approach Standard-Model levels. Unfortunately, both

	KTeV97	KTeV99	Improvement
Proton Intensity	3.5E12	8.0E12	2.28
Repetition Cycle	60 sec.	80 sec.	0.75
Beam Size	9.3 x 9.3 cm^2	11.0 x 11.0 cm^2	1.40
Beam Absorber	Out	Out	1.00
Detector Efficiency	0.83	0.91	1.1
DAQ Livetime	0.70	0.73	1.05
Run Time	11 weeks	9 weeks	0.87
Improvement (KTeV99/KTeV97)			2.40

Table 5: Factors of improvement from KTeV97 to KTeV99 for E799

modes suffer from the presence of the radiative Dalitz-decay backgrounds, $K_L \to e^+e^-\gamma\gamma$ and $K_L \to \mu^+\mu^-\gamma\gamma$. As we reach single-event sensitivities below 10^{-10}, we expect to have background from these processes, even after optimizing kinematic cuts. This means that the search for a signal will require a background subtraction, and further reductions in the 90% confidence-level upper limit will go as $\sqrt{N}$, rather than N.

To perform an accurate background subtraction, it will be essential to have a complete understanding of the radiative Dalitz backgrounds. As Table 6 shows, we expect to have a sample of about 2800 $K_L \to e^+e^-\gamma\gamma$ decays from the 1997 run of E799-II, compared to just 58 events from E799-I. It will be necessary to study carefully the kinematics of these events and their distribution in phase space in order to understand how effectively they can be removed by various cuts in the $\pi^0e^+e^-$ analysis. For this reason, the tripling of statistics that the 1999 run would permit would be invaluable.

When the $\pi^0e^+e^-$ and $\pi^0\mu^+\mu^-$ modes are observed, and their branching ratios measured, the task of separating the direct CP-violation part from the CP-conserving and indirect CP-violation parts requires still more information about other rare decays. In particular, to extract the CP-conserving amplitude for $K_L \to \pi^0e^+e^-$, a measurement of $K_L \to \pi^0\gamma\gamma$, including the $\gamma\gamma$ invariant mass spectrum, will be essential. Such a measurement will also provide information about the importance of $O(p^6)$ terms in chiral perturbation theory.

The next mode mentioned in the table is $\pi^0\nu\bar{\nu}$, using π^0 Dalitz decays. This mode is theoretically very clean, having no CP-conserving part, and there is no radiative Dalitz background. Of course, there are other backgrounds, and the sensitivity suffers due to the need to use the Dalitz decay to find a charged vertex. Nevertheless, the Dalitz-based analysis that can be performed with the standard E799-II beam configuration will provide useful cross-checks on the neutral analysis we also propose for the 1999 run.

The $K_L \to \pi^+\pi^-e^+e^-$ decay has been discussed previously, in Sections 2.3 and 2.4. This decay opens a new window on CP violation through the study of the final-state angular distributions. A very large asymmetry is expected due to the standard CP violation through mixing. The predicted asymmetry[9] in the integrated rate is between 13 and 14%; with the added statistics from the 1999 run the asymmetry could be measured to a precision of 1.2%, implying that we should see a 10-σ effect. In addition, various direct CP-violating terms can in principle be present in the amplitude for this decay. While these terms are not expected to

Decay Mode	Previous Experiments	Previous Exp. Results	KTeV97	KTeV97 + KTeV99
$K_L \to \pi^0 e^+ e^-$ SES 90% CL	E799-I [11]	1.8×10^{-9} $< 4.3 \times 10^{-9}$	8.3×10^{-11} In progress.	2.4×10^{-11} In progress.
$K_L \to \pi^0 \mu^+ \mu^-$ SES 90% CL	E799-I [24]	2.2×10^{-9} $< 5.1 \times 10^{-9}$	7.3×10^{-11} In progress.	2.1×10^{-11} In progress.
$K_L \to \pi^0 \nu \overline{\nu}$ SES $(\pi^0 \to e^+ e^- \gamma)$ 90% CL	E799-I [15]	2.5×10^{-5} $< 5.8 \times 10^{-5}$	1.2×10^{-7} In progress.	3.5×10^{-8} In progress.
$K_L \to \pi^0 \nu \overline{\nu}$ SES $(\pi^0 \to \gamma\gamma)$ 90% CL	None	- -	4.1×10^{-7} $< 1.6 \times 10^{-6}$	$\sim 2 \times 10^{-8}$ In progress.
$K_L \to \pi^+ \pi^- e^+ e^-$ $\delta\phi_{asym}$	None	- -	1800 events 2.2%	6120 events 1.2%
$K_L \to e^+ e^- e^+ e^-$	E799-I [25]	29 events $(4.0 \pm 0.8) \times 10^{-8}$	340 events	1160 events
$K_L \to e^+ e^- \mu^+ \mu^-$	E799-I [26]	1 event $(2.9^{+6.7}_{-2.4}) \times 10^{-9}$	12 events	41 events
$\pi^0 \to e^+ e^- e^+ e^-$	BNL [27]	146 events $(3.2 \pm 0.3) \times 10^{-5}$	7500 events	25000 events
$\pi^0 \to e^+ e^-$	BNL [28] E799-I [29]	21 events $(7.5 \pm 2.0) \times 10^{-8}$	200 events	680 events
$K_L \to e^+ e^- \gamma$	BNL [30] CERN [31]	1k events $(9.2 \pm 0.5) \times 10^{-6}$	120k events	408k events
$K_L \to e^+ e^- \gamma\gamma$	E799-I [32]	58 events $(6.5 \pm 1.3) \times 10^{-7}$	2800 events	9500 events
$K_L \to \mu^+ \mu^- \gamma$	E799-I [33]	197 events $(3.2 \pm 0.3) \times 10^{-7}$	7700 events	26000 events

Table 6: Expected single event sensitivity (SES), 90% CL on the branching ratio, the measured branching ratio or the number of events for various decay modes to be studied in KTeV.

be large in the Standard Model, the study of this mode provides another possible approach to observing direct CP violation that should be pursued. The 1999 E799-II run will allow us to do that.

A variety of electromagnetic decays are also listed in Table 6. The study of these modes can be used to check the radiative corrections to the lowest-order QED predictions, and also to measure the hadronic $K\gamma^*\gamma^*$ and $\pi\gamma^*\gamma^*$ form factors. These form factors are important inputs into a number of theoretical calculations, most notably that of the long-distance part of $K_L \rightarrow \mu^+\mu^-$. This mode has a short-distance component that could be used to extract the value of the CKM matrix element V_{td}, if the long-distance part were known. The absorptive part of the long-distance part can be calculated from the known rate for $K_L \rightarrow \gamma\gamma$, but the dispersive part requires accurate knowledge of the $K\gamma^*\gamma^*$ form factor, which can be gained only though a measurement of the double-Dalitz modes $K_L \rightarrow e^+e^-e^+e^-$ and $K_L \rightarrow \mu^+\mu^-e^+e^-$. The same connection exists between the $\pi^0 \rightarrow e^+e^-$ mode and the π^0 double Dalitz decay $\pi^0 \rightarrow e^+e^-e^+e^-$. It is interesting to note that E799-II will provide by far the largest sample of $\pi^0 \rightarrow e^+e^-$ decays by studying π^0 mesons produced in $K_L \rightarrow \pi^0\pi^0\pi^0$ decays.

The 1999 run will allow an improved study of numerous other decay modes. Among these are $K_L \rightarrow \pi^0e^+e^-\gamma$, where we expect to see hundreds or even thousands of events; $K_L \rightarrow \pi^0e^+e^-e^+e^-$ and $K_L \rightarrow \pi^0\pi^0e^+e^-$, where we will see only a handful and where the 1999 run will be critical. The decay $K_L \rightarrow \pi^0e^+e^-e^+e^-$ is important because it is sensitive to the dynamics of $K_L \rightarrow \pi^0\gamma^*\gamma^*$ which, as was mentioned above, is vitally important in order to understand the CP conserving amplitude that contributes to $K_L \rightarrow \pi^0e^+e^-$. The decay $K_L \rightarrow \pi^0\pi^0e^+e^-$ is the neutral partner of the previously mentioned $K_L \rightarrow \pi^+\pi^-e^+e^-$ decay, but does not include the CP-violating inner bremsstrahlung amplitude that is so important in the charged decay. A measurement of the neutral mode thus provides an independent way to disentangle the various amplitudes, as well as another opportunity to search for direct CP-violating phenomena.

The modes that we have discussed here give an indication of the increase in physics reach that the 1999 run of E799-II will achieve. Of course, we always hope for a surprise — an unexpectly large rate for a rare decay that signals new physics of some kind. In this vein, it is perhaps interesting to close this section by noting that a preliminary analysis of the E799-II one-day data sample from 1997 suggests that the sensitivity to the exotic, non-Standard model decay $K_L \rightarrow \pi^0\mu^\pm e^\mp$ achieved in 1997 will be competitive with Brookhaven experiment E-865, a dedicated search for the same kind of exotic couplings in charged kaon decays. This is just one of many E799 analyses that will provide valuable physics knowledge in addition to the fundamentally important searches for direct CP violation in the $K_L \rightarrow \pi^0l\bar{l}$ decay modes.

3.3 Hyperon Decays

Hyperon data taking will benefit from all of the improvement factors discussed in the previous sections as well as two additional factors. First, we made Ξ^0 trigger improvements between the first and second E799 running periods in KTeV97 which will be used throughout the 1999 run. Second, we propose to move the sweeping magnet (NM3S) upstream by 3 meters which will increase the usable hyperon flux by 19%. Table 7 is a summary of expected sample sizes for the Ξ^0 modes of primary interest. We are studying ways to reduce the hyperon level 1 trigger rates, including the effect of adding Y plane DC-or signals to the trigger. The large beta decay and radiative decay samples will provide precise asymmetry parameter measurements for these modes.

Decay Mode	Previous Experiments	Previous Exp. Results	KTeV97	KTeV97 + KTeV99
$\Xi^0 \to \Sigma^+ e^- \overline{\nu}$	None		900 events	4400 events
$\Xi^0 \to \Sigma^+ \mu^- \overline{\nu}$	None		$\sim$20 events	$\sim$100 events
$\Xi^0 \to \Sigma^0 \gamma$	FNAL [34]	85 events $(3.56 \pm 0.43) \times 10^{-3}$	4600 events	22500 events
$\Xi^0 \to \Lambda \gamma$	FNAL [35]	116 events $(1.06 \pm 0.16) \times 10^{-3}$	700 events	5000 events

Table 7: Expected number of events for various Ξ^0 decay modes being studied in KTeV.

Our interest in continuing the pursuit of Lambda beta decay, $\Lambda \to p e^- \overline{\nu}$, likewise remains strong. A Standard Model analysis of previous measurements with unpolarized Lambdas unambiguously predicts a neutrino asymmetry parameter value of $A_\nu = 0.974 \pm 0.004$ in polarized decays. Experiments with polarized Lambdas yield a measured value of $A_\nu = 0.821 \pm 0.060$, about 2.5 standard deviations lower than expected. Similar hints are also found in decay data for other polarized hyperons[36]. It is this suggestion of new physics which continues to intrigue and excite us. While the most conventional interpretation of such a difference would be in terms of a non-zero value for the "second class" form factor g_2, more exotic alternatives are certainly also possible [37]. A measurement in KTeV99 could reduce the experimental error by at least a factor of 3. Should this difference prove to be real, we could also explore its origin by examining other aspects of the decay angular distribution with high precision.

Given the proven performance of the KTeV detector in identifying electrons and reconstructing charged decays, the only significant experimental challenge which remains is the suppression of K_{e3} background by differentiating between high-momentum pions and protons (typical momentum 250 GeV/c) traveling in or near the neutral beam. During the 1997 run, the beam hole was instrumented with a first-generation TRD for the purpose of separating protons from pions at these momenta. Unfortunately, the high counting rate (1-2 MHz) in the beam hole region exceeded the rate capability of the parallel plate chambers and readout scheme which were employed [38]. An upgraded Beamline TRD system capable of providing the needed pion rejection (at least 50x) in such a high-rate environment is discussed in Section 4.8.

3.4 $K_L \to \pi^0\nu\overline{\nu}$ at KTeV99

We propose a dedicated run to search for the $K_L \to \pi^0\nu\overline{\nu}$ decay mode at KTeV99 using the decay $\pi^0 \to \gamma\gamma$. This decay is expected to be a purely direct CP violating mode. Therefore, observation of this decay mode near the predicted rate would provide unambiguous evidence for direct CP violation. The predicted branching ratio for this decay mode in the Standard Model is around 3×10^{-11}.

Considering the fact that the current best limit on this process is 1.6×10^{-6}, as discussed in section 2.4.2, five orders of magnitude higher than the predicted level, we believe that a programmatic, step-by-step approach will be necessary to achieve signal detection in our future program, KAMI. KTeV99 is an ideal opportunity to continue our studies of this mode with an eye toward the future. In this section we discuss in some detail the feasibility of achieving a sensitivity of 2×10^{-8} during the 1999 run.

3.4.1 Expected background levels at KTeV99

The expected sources of background for the $\pi^0\nu\overline{\nu}$ search are:

1. Beam neutrons interacting in detector material such as the vacuum window and drift chambers are expected to be the dominant source of background. These interactions can produce two or more π^0s, where two photons from different π^0s strike the CsI and misreconstruct inside the fiducial decay region while all other particles go undetected. This source of background was identified in a detailed analysis of the one day $K_L \to \pi^0\nu\overline{\nu}$ run since the submission of the KTeV99 LOI. This background is not expected to be a problem in KAMI since there will be no material in the beam upstream of the calorimeter[23].

2. K_L decays to $2\pi^0$ and $3\pi^0$ in which two and four photons, respectively, go undetected and the remaining two photons form two clusters in the calorimeter.

3. The decay $\Lambda \to n\pi^0$ combined with an accidental photon where one of the photons from the π^0 decay is lost.

4. The decay $\Lambda \to n\pi^0$, in which the the Λ originated from a Ξ^0 decay. These decays can be a serious problem since the final π^0 can carry a P_t as high as 230 MeV/c.

Beam neutrons which interact in the vacuum window or in the drift chambers can produce multiple π^0s. If two photons from different π^0s are detected in the CsI calorimeter, the reconstructed z vertex can be shifted into the fiducial decay volume. In order to minimize this possibility, the veto efficiency for all associated particles must be as high as possible. The current KTeV spectrometer has good charged particle veto efficiency using the drift chambers and the trigger hodoscope. Photons which miss the CsI and pass through the beam hole can be detected by the beam hole veto. Large-angle photons which miss the CsI calorimeter have a high probability of detection in the photon veto counters.

From a detailed study of the KTeV97 data (see Section 2.4.2), it is clear that beam interaction backgrounds can be reduced by increasing the efficiency for detecting the scattered neutron in the beam hole veto. The current beam hole veto detector consists of a 30 radiation length (~1 interaction length) sampling calorimeter designed primarily to detect high energy photons. Studies of the existing beam hole veto show that it has an 82% efficiency for neutron detection. This efficiency can be improved significantly with the addition of a hadronic calorimeter downstream of the existing beam hole veto.

The estimated background from events with a scattered neutron striking the beam hole veto during the $K_L \to \pi^0\nu\overline{\nu}$ special run was 3.5 ± 1.7 events; one background event was observed. If the neutron detection efficiency of the beam hole veto was increased to 99%, the expected background from this source would be reduced to 0.2 ± 0.1 for the same size data sample. This background estimate does not include beam interactions where the scattered neutron misses the beam hole veto and no other associated particles are detected. This component of the background is actively being studied in the data and using GEANT simulations of the detector.

An extensive Monte Carlo simulation was performed to determine the expected levels of background from K_L and Λ decays. The Monte Carlo events were generated with a configuration corresponding to the special 1996 run, i.e., with a 4x4 cm^2 beam size. All of the cuts used in the analysis of the 1996 $\pi^0\nu\overline{\nu}$ data were applied, and the number of events appearing in the signal search region, $160 < P_T < 260$ MeV, were counted in order to determine the background levels. The results of these studies are described in some detail in Appendix A.

The final background levels from the different decay modes after all cuts are listed in Table 8. With the exception of the beam neutron background, all other sources of background are expected to be negligible at a sensitivity of 1×10^{-8}. Detailed studies of the neutron induced background are currently underway. The background levels for the KAMI detector, which is explicitly designed to measure the decay mode $K_L \to \pi^0\nu\overline{\nu}$, are expected to be at the 1×10^{-11} level or below[23].

Decay Mode	SES of MC generation	Num. Obs. Events After Final Cuts	Background Level
nA $\to \pi^0$A			under study
$K_L \to \pi^0\pi^0$	6.5×10^{-10}	1	6.5×10^{-10}
$K_L \to \pi^0\pi^0\pi^0$	6.5×10^{-10}	1	6.5×10^{-9}
$K_L \to \gamma\gamma$	1.1×10^{-9}	0	$< 1.1 \times 10^{-9}$
$\Lambda \to n\pi^0$	1.4×10^{-10}	8	1.1×10^{-9}
$\Xi^0 \to \Lambda\pi^0, \Lambda \to n\pi^0$	7.5×10^{-12}	13	9.7×10^{-11}

Table 8: Expected background levels for the $\pi^0\nu\overline{\nu}$ search using $\pi^0 \to \gamma\gamma$ at KTeV99. These background levels correspond to a 4 cm $\times$ 4 cm beam at CsI, with the Be absorber in the beam.

3.4.2 Beam size

We intend to use the same beam size which was used during the special 1996 run (i.e. 4×4 cm^2 at the CsI). The kaon flux could be increased by using a larger beam, but the accidental activity in the detector would also increase. Accidentals contribute to the background and also result in the rejection of good events. A larger beam would also degrade our P_T resolution and further compromise our background rejection. For example, when Monte Carlo signal events are generated with a 6×6 cm^2 beam size in an accidental environment similar to that expected in KTeV99 for this beam size, the signal efficiency is reduced to 0.4%. The efficiency with 4×4 cm^2 beam is 1.25%, a factor of three increase. As a result, the gain in flux of 2.25 by increasing the beam size from 4×4 cm^2 to 6×6 cm^2 is nullified by the loss in acceptance.

By making the beam even smaller than 4×4 cm^2, one can gain even more in signal efficiency and P_T resolution, but the kaon flux goes down, requiring a longer run to achieve the same sensitivity. As discussed previously, our Monte Carlo background studies show that the existing P_T resolution corresponding to 4×4 cm^2 beam size is already adequate for the sensitivity we propose to achieve at KTeV99. The hadronic background level, which will be the limiting factor, is unaffected by the P_T resolution. As a result, a beam size of 4×4 cm^2 should be adequate for the 1999 run.

3.4.3 A γ-converter for $K_L \to \pi^0\nu\overline{\nu}$ detection

In the KTeV99 letter of intent, we discussed the possibility of using a γ-converter during the 1999 run. By converting one of the photons in a Scintillator-Pb-Scintillator sandwich situated just downstream of the vacuum window, we can ensure that the decay came from the vacuum region, thus reducing background from hadronic interactions. Studies described in detail in Appendix B show that the sensitivity of this technique is not competitive with the 2γ mode and hence, will not be pursued for KTeV99.

3.4.4 Running conditions and sensitivity

The single event sensitivity(SES)/week attainable during the 1999 run using a 4×4 cm^2 beam is summarized in Table 9, projected from the half a day of data taken in December 1996.

As described previously, this search will be limited by background from beam neutron interaction with detector material. To suppress this background in KTeV99, we propose to build a hadronic section for the beam hole veto which is capable of rejecting hadrons with an efficiency of 99%. This upgrade is necessary not only to reduce the background from beam neutron interactions, but also to reduce the background from Λ decays by detecting neutrons traveling in or near the beam hole.

	KTeV97	KTeV99	Improvement
Proton Intensity	3.5E12	8E12	2.28
Repetition Cycle	60 sec.	80 sec.	0.75
Beam Size	4.0×4.0 cm^2	4.0×4.0 cm^2	1.00
Beam Absorber	In	In	1.00
Acceptance	0.036	0.029	0.81
Running Time	11 hours	1 week (125h)	11.4
Improvement(KTeV99/KTeV97)			15.8
SES	4 x 10^{-7}	2.5 x 10^{-8}	

Table 9: Factors of improvement from KTeV97 to KTeV99 for $K_L \to \pi^0\nu\overline{\nu}$ with $\pi^0 \to \gamma\gamma$.

4 Beam and Detector Maintenance and Upgrades

4.1 Detector Maintenance and Upgrades for the 1999 Run

In the sections below, we describe several detector issues which must be addressed for KTeV to collect data as efficiently as possible in the 1999 fixed-target run. The upgrades proposed are designed to improve the reliability of the detector and to improve the trigger/DAQ livetime. The KTeV performance from the 96-97 run and our goals for the 1999 run are summarized in Table 10. The improvement in data-taking efficiency will come mainly from the replacement of CsI readout components, described in section 4.2. Several modifications to the trigger and front-end readout are required to achieve the livetime improvement; these modifications are described in Section 4.5. We estimate that the combined improvement will reduce the experiment's overall deadtime (i.e., total beam time for which the experiment is not live) by 30%, equivalent to adding 4.5 weeks to a 20 week run.

	KTeV97	KTeV99
Data-taking Efficiency (data-taking time / beam time)	0.80	0.90
Trigger/DAQ Livetime†	0.70	0.77
Overall Livetime	0.56	0.69

†Livetime for E832 assuming the same instantaneous beam intensity in 1997 and 1999.

Table 10: KTeV Data-taking Efficiency and Livetime

The improved slow-spill duty cycle (40/80 seconds instead of 20/60 seconds) will place increased demands on our data acquisition system. In Section 4.6, we describe necessary modifications to our DAQ system to cope with this new duty cycle.

4.2 Replacement of Custom Circuits in the CsI Readout

Failures of the custom integrated circuits that are central to the CsI readout system were the single largest source of data taking inefficiency during KTeV's 1996-97 run, accounting for half of the total inefficiency (20%). In addition, soft readout failures and the edge effects of hard failures compromised the quality of the data that was acquired. Reducing the frailty of these components is a principal goal of the KTeV99 upgrade, which will have the added benefit of reducing the manpower required to continuously monitor and repair the system.

The frequency of component failures grew to 2-4 hard failures per day of the 3100 channel system after 9 months of continuous operation. Each hard failure required access to the radiation enclosure for repair, which was a significant work load on the experimenters and beam operators. After nearly a year of essentially constant diagnostic work and studies (largely in parallel with the running time), it is now clear that the component failures are caused by out-of-specification fabrication problems of the integrated circuits by the vendor. The vendor (Orbit Semiconductor) has acknowledged these problems, and has refabricated the DBC chips once already and is in the process now of refabricating the QIE chips at no cost to the laboratory.

Based on failures and subsequent studies that occurred after the first refabrication of the DBC chips, it is clear that the DBC chips will have to be refabricated a second time. We are now negotiating with the vendor to fully cover the capital costs associated with refabricating the DBC chips again. If the vendor agrees to fully cover the costs of the second DBC fabrication, then the estimated remaining capital cost of replacing the QIE and DBC custom chips will be \$40k, and five man-months of surface-mount component technician time. If the vendor is not willing to cover the estimated \$110k total refabrication cost, then the cost of the chip replacement project could be as large as \$165k. These negotiations are ongoing, and one outcome could be that the vendor and laboratory split the cost of the second fabrication of the DBC chips. In this scenario the capital cost to the laboratory for chip replacement would be \$110k. Additional maintenance costs for the CsI blockhouse and CsI readout system is estimated to be \$10k. The various cost scenarios are listed in Table 11. We have assumed the middle budget scenario for planning purposes.

Task	Orbit pays DBC fab.	Orbit/FNAL split DBC fab.	FNAL pays DBC fab.
Failure Diagnostics	\$5k	\$5k	\$5k
QIE fabrication	—	—	—
DBC fabrication	—	\$55k	\$110k
QIE & DBC replacement	\$40k	\$40k	\$40k
Blockhouse maintenance	\$5k	\$5k	\$5k
General Readout maintenance	\$5k	\$5k	\$5k
Total	\$55k	\$110k	\$165k

Table 11: Capital costs to Fermilab of CsI calorimeter maintenance for three cost scenarios.

4.3 Drift Chamber and TRD Maintenance and Operation

During the 1996/97 fixed-target run, our most upstream drift chamber suffered substantial radiation damage. Near the beam region of the chamber, the minimum ionizing pulse height was reduced by 30% as a result of the radiation damage. Because of this damage, about half of that chamber will need to be restrung before the 1999 fixed-target run. A second chamber, which exhibited some current draw at various times during the run, will need to be cleaned. For these efforts, we will need access to a clean-room facility. Some help from the technician staff in Lab 6 will likely be needed together with summer students from the universities and Fermilab. In addition to manpower needs, we will have some modest needs in terms of equipment and supplies.

We have started an R&D effort with a full length, 1/10 width test chamber to study parameters that could be related to inefficiencies and radiation damage observed during the run. Pre-amplifier and post-amplifier performances, gas mixtures, alcohol content of the Argon/ethane mixture, radiation damage limits, interconnect cables, and related environmental noise will be studied. It is not clear at the current time what improvements will be made, but it is likely that all parameters will be better optimized for the 1999 run. For example, the value of the current limiting resistors in the beam regions may be reduced to minimize voltage sag in these high current regions.

The helium bags are an integral part of the chamber system, since they fit within a few centimeters of the chamber windows. The reduced multiple scattering in the material is one of the main improvements realized by KTeV over previous experiments. Although the helium bags worked well in reducing the multiple scattering, they leaked badly. We would like to replace them with bags which are more gas-tight, similar to those used by Fermilab experiment E815. The helium gas costs in the 1997 run totaled $58k. We expect that we can reduce these costs significantly with this better design. The savings in helium alone will more than justify the expense of new helium bags.

The TRD chambers and recirculating xenon gas system performed well during the run and typically delivered π/e rejection of 150:1 with a 90% electron efficiency. During the run, the system requires some basic maintenance such as daily gas chromatography data taking and high voltage feedback control. Before the 1999 run, two TRD chambers may need to be opened to fix broken printed circuit board traces; this repair should not take more than 2-3 days of work.

The estimated costs for the drift chamber and TRD systems are listed in Table 12.

4.4 Total Energy Trigger Maintenance

During the installation of the total energy trigger (ET) the system overheated due to problems with the KTeV Hall HVAC system, and comparator chips on the boards were severely damaged. The ET system provides inputs to the cluster counter which is part of the level 2 trigger. Damage to these comparators results in noisy inputs to the cluster counter. During the past run we replaced 1168 of these comparators. There are an additional 2416 comparators which have not been replaced. While only a small number of the remaining comparators exhibit noisy behavior, our experience indicates that those comparators which have not been swapped will eventually become noisy. Unless they are replaced, we can expect continued

Item	Cost
Wire for DC1 restringing	\$3.5k
Miscellaneous supplies and equipment	\$2k
New He bags	\$7k
Second transfer frame for restringing DC1	\$1.5k
MVL407 discriminator chips (spares)	\$1.2k
Single electron efficiency improvements	\$30k
Drift chamber gas	\$11k
Helium gas †	\$29k
TRD gas	\$4k
Total	\$89.2k

† Assuming a leak rate which is half of the 1997 rate.

Table 12: Drift chamber and TRD cost projections for the 1999 run.

failures during the KTeV99 run along with a decrease in data-taking efficiency due to down time for repairs. We propose to improve the reliability of the ET system by replacing the remaining 2416 comparators. At \$5 per comparator, this repair will cost approximately \$12k, and will require about 2 man-months of surface mount technician time. Precautions have been taken to prevent any further overheating of the ET system.

4.5 Trigger and Front-end Electronics

4.5.1 Sources of dead-time

We have studied data from the 1997 KTeV run to understand sources of dead time in the trigger and readout, and to investigate ways to reduce the dead-time in the 1999 run. The trigger/readout live-time was about 70% in the E832 run, and about 65% in the E799 run. This section will focus on identifying sources of dead-time in KTeV, and then make proposals for improvements.

In E832, roughly 3/4 of the dead-time was contributed by the front-end readout, and the remaining 1/4 was from the level 2 trigger. In E799, the dead-time contributions from the front-end readout and the level 2 trigger were nearly equal. The level 3 filter was 100% live in both E832 and E799. Therefore, to reduce deadtime, we need to make improvements to both the front-end and the trigger, although the front-end improvements are more important for E832.

There are two main sources of readout dead-time. The first is from the FERA (Fast Encoding Readout Architecture developed by LeCroy) ADC readout, especially for high occupancy detectors like the beam hole veto and the regenerator, both of which are in the beam. The FERA readout time is 8.7μs for digitization, plus an additional 100 ns for each channel which is read out. The second limiting source of readout dead-time is from the pipeline latches that read out level 2 trigger information. These latches cannot begin digitization until a level 2 signal is received, which arrives 2-3 μs after the level 1 signal. The dead-time for these latches is 12 μs, plus 100 ns per word.

The main source of trigger dead-time is the Hardware Cluster Counter (HCC), which takes close to 3 μs to make a decision. This is about 1 μs longer than the other level 2 processors.

4.5.2 Front-end upgrades

The most obvious way to reduce the FERA readout dead-time is to reduce the occupancy by raising the readout thresholds. We plan to do this for both the beam hole veto and the regenerator. Since no new hardware or software are required to raise the thresholds, the final decision will be made after a more detailed analysis of the current data.

Another improvement is to reduce the FERA digitization time by modifying the ADCs to give 8-bit precision instead of 10-bit precision. This modification is expected to reduce the readout time by ~ 3 μs. We have studied the physics impact of losing two bits of ADC information, and find that we need two types of ADC as shown below in Table 13.

The (non-TRD) ADC requirements are set by our need to calibrate with muons. Almost all of the detectors give ~ 100 count muon signals with the current 10-bit digitization. By keeping the same dynamic range with 8-bit precision, MIP signals will give ~ 25 ADC counts, which is still sufficient for calibration. Studies of the TRD show that the rejection is the same using 8-bit and 10-bit digitization, provided that the dynamic range is maintained.

For the beam hole veto and the Collar-Anti (CA), a MIP signal results in about 5-10 ADC counts with the current 10-bit digitization; thus we cannot afford to lose precision here. However, the dynamic range for the beam hole veto and CA is about one order of magnitude larger than our off-line cut, which means that we can afford to lose a factor of four in dynamic range.

Precision	Detectors	LSB	No. of modules
8-bit	Reg, MA, RC, SA VV', HA, Mu2, Mu3, TRD	1 pC/count	172
8-bit	BA, CA	1/4 pC/count	10

Table 13: The two types of proposed FERA ADC modules are matched to the appropriate KTeV detectors.

Another significant readout upgrade is to replace the three pipeline latches used for level 2 trigger information. Since the level 2 information is latched, we do not need the pipeline latch capability of reading out eight consecutive RF-buckets. Instead we plan to use a modified version of the custom FERA Crate Trigger Interface (CTI) module, which will effectively readout just one RF-bucket. This will reduce the dead-time in the trigger-latch crate by about 4 μs.

The last potential source of dead-time comes from reading out the level 2 processors (hardware cluster counting and drift chamber hit counting). These processors were built with internal event buffering to reduce the dead-time from reading out high-occupancy events.

The problem is that the CTI, which transfers the data to the FERA Readout Controller is not buffered. As a result, the buffering in the level 2 processors was disabled in the 1997 run. If we run the same way at higher beam intensities in 1999, this could cause additional dead-time. For the KTeV99 run we plan to build a new CTI which is buffered.

4.5.3 Trigger upgrades

Three hardware upgrades for the trigger system are proposed for the 1999 run. The first upgrade is to reduce the Hardware Cluster Counter (HCC) calorimeter trigger decision time from 3.0 to 2.4 μs. This will be done by replacing the HCC master clock, and reprogramming one of the Programmable Logic Devices (PLD) in the HCC controller. In addition to reducing the HCC level 2 processing time, we are studying the impact of the FERA CLEAR time, which we would like to reduce from its current value of 500 ns down to 200 ns. This modification requires no additional hardware or software, but may require studies of the FERA ADC pedestals at high rates. And lastly, we would propose to address rate effects observed in the drift chamber trigger sources. These rate effects arose from inductive coupling of the drift chambers to the global trigger system. We propose to replace the inductive coupling circuits with optical coupling circuits which will be immune to these rate effects.

4.5.4 Net live-time improvement and cost

Making reasonable assumptions, the expected live-time improvements for E832 are shown in Table 14. In total, we expect a 10% increase in yield when running at the same instantaneous intensity. Comparable yield improvements can be expected for E799, although the final degree of improvement will depend on details of the trigger configuration which are currently under study. The estimated costs are given in Table 15. This table also includes the cost of spare modules for the TRD trigger system.

Change		Increase in Live-time
HCC:	3.0 $\mu s \rightarrow$ 2.4 μs	+2%
Clear Time:	500 ns $\rightarrow$ 200 ns	+1%
Readout Time:	17 $\mu s \rightarrow 12\mu$s	+7%
Total:		+10%

Table 14: Estimated live-time improvements for E832 after making the proposed trigger/readout upgrades.

4.6 Data Acquisition System

4.6.1 Online system

The improved slow-spill duty cycle (40/80 seconds instead of 20/60 seconds) and the higher intensity planned for the 1999 fixed-target run will place increased demands on our data

Item	Qtty	Cost
reduce HCC processing time	2	\$4.4k
Modify FERA (10-bits to 8-bits)	187	\$1k
1-slice latch (modified CTI)	7	\$15k
Buffered CTI for readout	12	\$6k
Optical coupling electronics for the drift chamber trigger	6	\$2.4k
TRD trigger spares	4	\$6.4k
Total		\$35.2k

Table 15: Projected costs for trigger/front end upgrades.

acquisition system. We have used data from the 1997 run to estimate the DAQ requirements for 1999 conditions.

The 1997 run used a data acquisition system[39] provided by DART, a project within the Fermilab computing division. Data was read out over a FERA bus into VME memory modules using DART specific hardware (DYC, DC2) and software. Once in VME memory, the data were read into Challenge L computers, the KTeV level 3 farm, using a commercial (Performance Technologies) VME to VME interface. The driver for this interface was written and supported by DART. Other DART software read and formatted the data to send to the KTeV level 3 reconstruction and analysis package, buffered and formatted data coming out of the level 3, and wrote the data to DLT tape as well as disk.

The KTeV level 3 farm consists of 4 Challenge L servers, 3 of which are used to filter events and 1 which is used to monitor data quality and perform online calibrations required for the level 3 filter. The 3 filtering computers each have eight 200MHz R4400 processors. The monitoring computer has ten 150MHz R4400 processors.

4.6.2 DAQ hardware upgrades

Table 16 shows the relevant DAQ parameters for the 1999 run, scaled from 1997. For the E832 estimate, the scaling was done using an E832 run with an average SEM of 2.9×10^{12} scaled to 1999 conditions with an average SEM of 8×10^{12} and a 40 second spill. For the E799 estimate, the scaling was done using an E799 run with an average SEM of 3.0×10^{12} scaled to 1999 conditions with an average SEM of 8×10^{12} and a 40 second spill. The livetime improvements quoted in Tables 4 and 5 have been included.

As shown in Table 16, the available input memory and output rate capability are sufficient (barely) for the 1999 run, but more CPU power will be needed. Based on the extrapolation from 1997 data, and considering the additional CPU requirements of online splitting (described below), we estimate that the CPU power of the three filter Challenges should be increased by 50%. The cheapest method of increasing the CPU by this amount is to purchase 6 R10000 processors.

The level 3 Challenges each have 256 MB of internal memory. We need to double this memory on the monitoring plane, which ran at the memory limit during 1997. This memory shortage limited our ability to monitor the detector. The increase of CPU on the filtering

	1997	1999	Available
Input data volume (E832)	1111 MB/spill	3196 MB/spill	4032
Input data volume (E799)	1180 MB/spill	3282 MB/spill	4032
Output data volume (E832)	281 MB/spill	808 MB/spill	1000 MB/spill
Output data volume (E799)	177 MB/spill	493 MB/spill	1000 MB/spill
$< \text{CPU} >$ / spill (E832)	28 seconds	81 seconds	80 seconds
$< \text{CPU} >$ / spill (E799)	31 seconds	86 seconds	80 seconds

Table 16: DAQ parameters scaled to 1999 run

planes means that we will be running 50% more filter processes on each plane (12 processes instead of 8). The impact of more filter processes on available memory needs to be studied, but we believe it will be necessary to increase the memory on the filter planes as well.

4.6.3 Online splitting

During the 1999 run, KTeV typically wrote data to 9 DLTs simultaneously. Each of these tapes included the same mix of trigger types. Before beginning to analyze large samples of data, it is necessary to "split" these raw data tapes into tapes containing different classes of events. This splitting process has required significant manpower and computing resources; it has also required us to double the number of tapes purchased since the split tapes form almost a complete copy of the original tapes.

For the 1999 run, we plan to eliminate the offline splitting process by writing "split" tapes directly from our online system. Producing split tapes online will substantially reduce our tape requirements for the 1999 run, saving approximately $150k of DLT tapes, and will eliminate the long delay to analysis caused by offline splitting. Eliminating the offline split will also leave offline resources free for analysis of 1997 as well as 1999 data.

In our current system, the level 3 system writes selected events directly to tape. For 1999, events will be first written to disk files containing single classes of events (e.g., $K_L \to \pi e \nu$ candidates). A separate process will copy these disk files to tape. This scheme requires that we add additional disk space to our cluster to buffer events, and that the network connection among the online machines be upgraded so that we can copy event files across the cluster. We plan to add 300 GB of disk which will allow us to buffer about 8 hours of data. During smooth running, much less buffer space will be required; the 8 hour buffer will allow us to deal with tape problems without having an effect on data-taking. The network will be upgraded from the current switched ethernet to either 100 BaseT ethernet or FDDI. Finally, we plan to add an additional DLT drive to each Challenge to provide a hot spare for each machine. Note that the $90k hardware cost related to online splitting (see Table 17) is more than offset by the ~$150k savings in DLT tapes.

We are currently carrying out a series of tests to demonstrate the technical feasibility of the online splitting plan and to choose a network technology. Critical issues include bandwidth of simultaneous reading and writing to a disk and network performance when spooling data from a remote disk to a DLT.

We will need DART software support for online splitting, including software to spool data off disk and onto tape, databasing of which runs and types of events are written on which tapes, deleting runs once they are spooled, and requesting new tape mounts as needed.

4.6.4 Slow DAQ upgrades

The KTeV Slow-DAQ system[40] was designed to interface with all the KTeV CAMAC crates, as well as monitoring temperatures, humidities, and voltages for the CsI and other detectors. Two SGI Indy machines, with SCSI-CAMAC interfaces supported by DART (the Jorway), were used to interface with the CAMAC crates. The time to initialize the CAMAC system for a new run was about 5 minutes. For the 1999 run we would like to modestly upgrade the Slow-DAQ system both to reduce the initialization time by a factor of 2 and to make the system more robust. The bottle neck of the Slow-DAQ was the serial CAMAC system. In the 1997 run, we operated 3 serial branches, running from the SCSI I/O port of one SGI Indy (atev1), serving a total of 73 CAMAC crates. These branches are:

1. the level 1 and level 2 trigger branches, which consist of 23 CAMAC crates located in the counting room;

2. the FERA ADC and TRD gas system branch, which consists of 24 CAMAC crates located in the counting room;

3. the Detector Hall Branch, which consists of 26 CAMAC crates in the detector hall.

A big portion of the CAMAC bandwidth is used to monitor the LeCroy 1440 High Voltages for the CsI and the CAEN high voltages for the TRD system which were both in the detector Hall CAMAC branch. We would like to remove the CsI HV monitoring from the system completely, and make a separate system for this task using an additional SGI Indy with a SCSI-CAMAC interface. An alternative solution would be to run the CsI LeCroy 1440 HV monitoring through the serial interface of a dedicated PC running Linux since the LeCroy 1440 system provides such an interface.

Next we plan to split the remaining monitoring on the detector Hall branch into two serial CAMAC branches with about 13 CAMAC crates in each branch, and run one of these branches from the SCSI I/O port of the second (existing) SGI Indy (atev2). The communication between the SCSI serial branches in the different machines (atev1 and atev2) will be done with the help of the RCAM product (remote CAMAC) which is supported by DART. Thus, we will be running a total of four serial CAMAC branches, two being in the counting room and other two being in the detector hall. An additional 300 feet of CAMAC RS-422 cable will be needed for the new CAMAC branch.

4.6.5 Continued DART support

We assume that DART will continue to support the hardware and software developed for the 1997 run until the completion of the 1999 run, and provide consulting to KTeV to upgrade the rest of the KTeV online system to the new versions of tools and operating systems. In particular, the following items will need to be addressed:

1. Operating system upgrades to the currently supported version of IRIX, at least IRIX 6.2 and probably higher. This will involve porting all DART software, understanding and tuning the new kernel parameters, and rewriting the VME to VME drivers.

2. Possibly replacing VME to VME interfaces. Performance Technologies no longer supports VME to VME interfaces. Depending on how many spares there are at the lab, we may need to buy different interfaces. We use a total of four such VME to VME links (8 modules). In addition, new drivers would have to be written.

3. Upgrades to VxWorks 5.3 operating system. Wind River no longer supports VxWorks 5.2 and no longer supports IRIX as a cross development platform for VxWorks 5.3 and beyond.

4.6.6 Online alarm system

During the 1997 run, we implemented an audio alarm system which alerted the shift crew to problems with the output from the level 3 trigger and online monitoring system. This system was implemented in the middle of the run and lead to an increase in data quality. During 1997, this system was mainly used to detect failures of the CsI electronics (see Section 4.2). For the 1999 run, we plan to rewrite the audio alarm system to add more flexibility and allow the system to monitor the whole detector. We expect that this work will require approximately 1-2 man-months of effort. The upgraded alarm system will both increase the data quality of the upcoming run and reduce the load on the shift crew.

4.6.7 DAQ upgrade costs

Table 17 shows cost estimates the DAQ upgrades described above.

Item	Description	Cost
Upgrades for 40/80 Duty Cycle		
CPU	6 R10000 CPUs	$90k
SGI memory	256 MB → 512 MB	$28k
Online Splitting		
Networking	4 FDDI/Challenge interfaces	$24k
	KTeV hall networking	$20k
Disks	300 GB	$30k
DLT drives	4	$16k
Slow DAQ Upgrade		
SGI Indy	1	$10k
RS-422 Cable	300 ft.	$1k
Total		$219k

Table 17: Cost estimate for the 1999 DAQ upgrade

4.6.8 DLT tapes

Our data storage requirements for raw data will total about 50 Terabytes, corresponding to about \$150k of DLT tapes. As mentioned above, without online splitting another ~50 Terabytes of tape would be required for split data.

4.7 Detector Upgrades for $K_L \to \pi^0 \nu\overline{\nu}$

In the KTeV99 Letter of Intent, we proposed several detector upgrades to help reduce backgrounds to $K_L \to \pi^0 \nu\overline{\nu}$, including upgrades to the beam hole veto, an additional upstream photon veto, a charged veto, and a gamma converter. Extensive studies since the submission of the LOI have shown that, with the exception of the beam hole veto, these upgrades are unnecessary in light of the beam neutron interaction background (see Section 2.4.2). In the following sections, we describe the proposed upgrade to the beam hole veto. The upgraded electromagnetic section of this device is a KAMI prototype detector designed to provide efficient photon detection in the presence of a high neutron flux. The new hadronic section of the beam hole veto will allow us to reduce the beam neutron interaction background, as well as hyperon decay backgrounds.

The need for upgraded photon veto detectors to isolate $K_L \to \pi^0 \nu\overline{\nu}$ decays in KAMI has been described in detail in the KAMI EOI[23]. We propose to study various photon veto technologies for KAMI at the INS facility at KEK. These tests are described in Appendix C.

4.7.1 KAMI beam hole veto prototype

The Electromagnetic section of the beam hole veto is necessary to detect photons which pass through the CsI beam holes from $K_L \to 2\pi^0$ and $3\pi^0$ decays. It covers the largest acceptance of all the photon vetos, and it must operate in an environment with a significant neutron flux. Under the conditions described earlier for the 1999 $\pi^0 \nu\overline{\nu}$ running, the beam hole veto is expected to see a neutron flux of about 1 MHz. Thus, we plan to veto every possible interaction in the beam hole veto. This would result in an efficiency loss of less than 5% for the signal.

During the KAMI era, the neutron flux is expected to exceed 100 MHz. For comparison, the expected kaon and neutron flux at KTeV and KAMI under various conditions are listed in Table 18.

	Beam Configuration	Kaon Flux	Neutron Flux
KTeV97	$\pi^0 \nu\overline{\nu}$ special run	0.3 MHz	0.7 MHz
	Nominal E799 running	12 MHz	44 MHz
KTeV99	$\pi^0 \nu\overline{\nu}$ run	0.6 MHz	1.2 MHz
	Nominal E799 running	18 MHz	70 MHz
KAMI-Far	KAMI $\pi^0 \nu\overline{\nu}$ running	28 MHz	200 MHz
KAMI-Near	KAMI $\pi^0 \nu\overline{\nu}$ running	110 MHz	550 MHz

Table 18: The kaon and neutron flux at KTeV and KAMI for various beam configurations.

For KAMI it becomes critical to design a beam hole veto which is neutron transparent, yet has high rejection power for photons. One way to achieve such rejection is through fine-grained depth segmentation, with active sampling every 2-3 radiation lengths. The energy threshold on each individual section can be tuned to maximize photon rejection and to distinguish photons from neutrons. Fast timing resolution is also useful to distinguish out-of-time neutron interactions, once the beam is debunched as expected for KAMI. For this reason, we plan to replace the plastic scintillator in the existing beam hole veto with a Cherenkov medium. Due to the high radiation level, the number of possible materials is very limited. Fused silica is known to be radiation hard, and we are currently considering this as a leading candidate.

The current beam hole veto is segmented every 10 radiation lengths in depth and has a total of 30 radiation lengths. To achieve much better discrimination of photons from neutrons, we plan to reduce the number of lead sheets by half (15 radiation length total) and increase the depth readout segmentation from three to six. Table 19 summarizes the proposed modifications.

	Existing beam hole veto	Proposed beam hole veto
Total Depth	$30X_0$	$15X_0$
Depth of each section	$10X_0$	$2.5X_0$
No. of sections	3	6
Thickness of Pb	2.7 mm ($0.5X_0$)	2.7 mm ($0.5X_0$)
Active medium	3HF Scint.	Fused silica
Thickness of Active medium	2.5 mm	7.7 mm

Table 19: Comparison of the EM sections of the existing beam hole veto and the proposed beam hole veto for KTeV99.

These modifications can be achieved using the existing beam hole veto mechanical structure. One Pb sheet plus two scintillator sheets will be replaced by a thick fused silica bar. The light guide needs to be modified for better depth segmentation accordingly. Such a beam hole veto allows us to fully test its functionality in a realistic beam environment during the KTeV99 run.

4.7.2 Hadronic section of the beam hole veto

As shown in the background study in Section 3.4.1, the inclusion of a new hadronic section of the beam hole veto is useful to detect not only the hadrons from neutron interactions but also the neutrons from lambda and cascade decays.

We have identified a candidate for such a hadron calorimeter which was previously used in FNAL-E687. The E687 beam calorimeter consists of 16 layers of depleted uranium plates (3.81 cm thick, 41 cm by 41 cm), each reinforceed by steel plates (0.238 cm thick) on both sides. Each layer corresponds to 0.4 nuclear interaction lengths, for a total depth of $0.4 \times 16 = 6.4\ \lambda_0$. The current mechanical structure has a 1.8 cm gap between the depleted uranium plates which allows for the insertion of an active medium, which will be either a

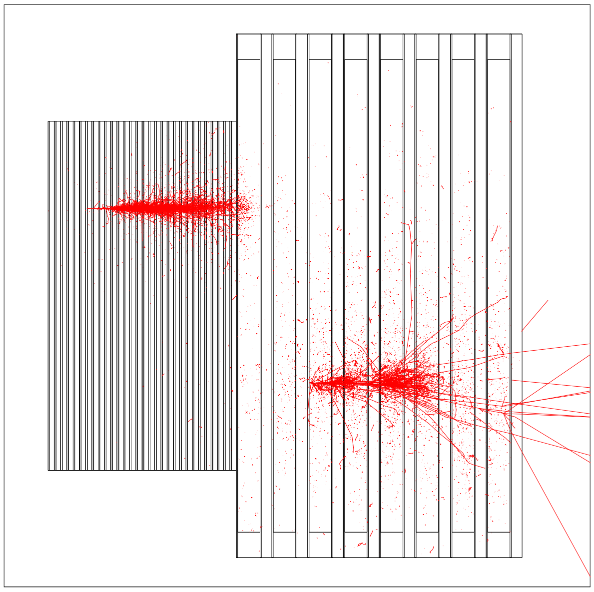

Figure 15: Typical photon and neutron interactions in the proposed beam hole veto. The top event shows a 30 GeV photon interacting in the EM section of the modified beam hole veto. The bottom event shows a 100 GeV neutron interacting in the hadronic section.

Cerenkov radiator or plastic scintillator. We plan to re-assemble the absorbers into two sets of 8 layers each so that both sides of the beam hole region can be covered. Figure 15 shows a plan view of the beam hole veto detector with the proposed hadronic section installed. A typical interaction of a 30 GeV photon and a 100 GeV neutron generated by GEANT are shown as well.

The hadronic section will be located behind the EM section of the beam hole veto. GEANT simulations show that the combination of the EM section with the newly proposed hadronic section results in a neutron detection efficiency of 99.0% with a 10 MeV energy threshold in the active medium, and a 98.4% efficiency even with a 30 MeV energy threshold.

Table 20 shows the cost estimate for the beam hole veto for both the EM and Hadronic sections.

4.8 Beamline TRD

As discussed in Section 3.3, a Beamline TRD to reject background pions from K_{e3} decays is necessary if we are to take advantage of our unique capability to investigate the suggestion of new physics in polarized $\Lambda \to pe^{-}\overline{\nu}$ decays.

A rather complete published report[41] describes the successful use of a TRD system in Fermilab experiment E769 to separate pions and protons in a 250 GeV/c incident charged hadron beam at "rates up to, and sometimes even exceeding, 2 MHz". While this 24-module TRD system had an extremely high *intrinsic* rejection, it was limited in their particular application to about 50:1 by the presence of untagged background tracks (at about the 2% level), by gain variation due to space charge effects in the dense central beam region, and by loss at high intensities of the excessively thin (14 nm) aluminum coating on the mylar

Items	Cost	Subtotal
Beam hole veto, EM section		
Fused silica bars	\$55K	
Light guide	\$10K	
Mechanical modification to beam hole veto	\$10K	
		\$75k
Beam hole veto, hadronic section		
Scintillator	\$10k	
Light guide	\$5k	
Support frame	\$5k	
PMT and readout electronics	\$10k	
		\$30k
Total Cost		\$105k

Table 20: Cost estimate for the beam hole veto upgrade.

cathodes. All three problems can be readily obviated in our application. Note, in particular, that stray tracks cause us no serious problem. They simply result in a uniform proton loss which can be made to cancel in branching ratio calculations and which will not bias our angular distributions.

Each of their TRD modules consisted of a 200-foil radiator followed by a PWC with two gaps and sense planes. The chambers were based on the prototype design for the Fermilab beam PWC ("Fenker chamber")[42] with a 1 mm wire spacing, a 6.35 mm cathode separation, and a collection time of about 100 ns.

It is possible to extract the basic measured module performance parameters from the article (apart from the operational limitations discussed above). They quote an 8.2% average efficiency for each chamber gap to detect a minimum ionizing particle which produces no transition radiation (proton). They also quote 18.8 for the measured average number of chamber gaps (out of 48) which fire in response to a 250 GeV/c pion (compared a predicted number of 20). This implies an average hit probability per chamber gap of $(18.8/48) = 0.392$, with distinct probabilities of $P1 = 0.46$ for the first gap after the radiator and $P2 = 0.32$ for the second gap.

Employing a simple hit-counting algorithm and computing combined binomial distributions with these probabilities indicates that a 10-module system with these parameters would meet our requirements. For example, requiring <4 hits corresponds to a pion rejection of 53 with a proton efficiency of 92%. Of course, higher rejection can be obtained at the expense of lower proton efficiency. Somewhat better performance could be achieved with a likelihood analysis which takes account of the differing hit probabilities for the first and second gaps. With a 100 ns collection time, the TRD signals can also be used to reduce the Level 1 trigger rate and associated dead time. For instance, rejecting triggers with more than 8 hits would reduce the trigger rate by about 1/2.

Chambers derived from standard 128-wire Fermilab sense planes[42] with aluminized

Mylar cathodes would provide a sensitive area appropriate for our decay protons. During KTeV97 we began preliminary studies of Fenker chamber performance in the neutral beam environment. Scaling from reference [41], the 10-module system would be 1.2 m long which would fit in the available space. Radiators of suitable size, fixturing and materials for making the aluminized Mylar cathodes (with 85 nm Al coating), and appropriate high voltage supplies already exist at The University of Chicago. Table 21 provides a cost estimate summary. We assume that chamber wires are ganged together in sets of four before amplification, and that each chamber gap is read out in 8 segments (each segment corresponding to 16 wires) to reduce randoms losses. Materials and instrumentation are included for two complete spare modules. This instrumentation scheme would require 352 latch channels, 44 ADC channels, and 44 logical OR channels to serve as trigger inputs. We request that these electronics modules be provided by the Fermilab PREP pool.

Item	Cost
44 metal chamber frames	\$2.2k
44 chamber wire frames	\$2.2k
1410 amplifier channels	\$28.2k
Gas consumption	\$4.0k
Total	\$36.6k

Table 21: Beamline TRD cost projections for the 1999 run.

This Beamline TRD system design is presently at a conceptual stage, so cost estimates given here are preliminary. Efforts to arrive at a fully optimized design are under way. We are searching for additional collaborators and technician help to realize the promise of this detector system. A program of additional design calculations and lab tests of X-ray detection with a Fenker chamber has begun at The University of Chicago.

4.9 Primary Beam Maintenance and Upgrades

During the 1997 run, the primary beam position was monitored with SWIC and SEED chambers in the beam. The total proton flux of the proposed 1999 run would exceed the integrated charge limit of the SWIC chambers. We propose to augment the in-beam SWIC and SEED instrumentation with non-invasive BPM readout technology which presents no material to the beam. The BPM electronics costs about \$3k/unit for 6 units and requires 6 man-months of engineering effort (the same effort as is needed for PWest). The ceramic boards used in the SEEDs need to be replaced at a total cost of about \$6k. The automatic beam tuning software will have to be modified to interface to the new site-wide beam control system. During the summer months the target hall service building would frequently overheat which was a cause of beam down time. Air conditioning needs to be installed in this building to keep the temperature controlled. We would also propose that a small toroid be installed in the primary beamline for absolute beam intensity measurements at a cost of \$5k.

Item	Cost
New BPM electronics.	\$18k
New SEED boards.	\$6k
Toroid	\$5k
Total	\$29k

Table 22: Primary Beam Maintenance and Upgrades.

4.10 Neutral Beam Line Modifications

Three beam sizes will be required for the 1999 run; 9.3 x 9.3 cm^2 for E832, 11.0 x 11.0 cm^2 for E799 and 4.0 x 4.0 cm^2 for $\pi^0\nu\overline{\nu}$. These three beam sizes can be implemented with different inserts in the final collimator. The final collimator is made with a large outer shield and a carefully machined insert which can be changed in 1-2 shifts. Inserts for the 9.3 x 9.3 cm^2 and 11.0 x 11.0 cm^2 beam sizes were employed in the 1997 run and can be used again in the proposed run. The small 4.0 x 4.0 cm^2 beam size that was used in the one-day $\pi^0\nu\overline{\nu}$ run was realized with movable jaw collimators that were upstream of the final collimator. We expect that the beam halo for the small beams would be reduced by using the final collimator to define the beam. This would require the fabrication of an additional set of inserts for the small beams at an estimated cost of \$15k. Some modest engineering resources would be required to design these inserts.

4.11 Vacuum System Maintenance and Window Replacement

There are a number of maintenance and upgrade issues associated with the KTeV Vacuum System and regenerator mover. The necessary maintenance costs sum to \$33k. These maintenance issues are listed below. Of critical importance are two months of skilled vacuum technician time for the necessary maintenance.

1. Replace broken vacuum valve. One of the valves in the fore-system failed during the last run. It was blanked off as a 'quick fix'. This valve must be replaced. The estimated cost is \$8k.

2. Regular large vacuum window replacements will continue. Before running, the current window must be replaced. The window exists. During running, there will probably have to be another scheduled replacement. Materials exist, but appropriate manpower must be identified.

3. The seals on the blower pumps must be replaced. Both blower pumps are leaking oil at an unacceptably high rate. It is unlikely we could run the system without replacing the seals. The seals are currently on hand. Identifying the required vacuum technician is again an issue. It is likely the pumps will have to be reconditioned at the factory with an estimated cost of \$20k.

4. The regenerator mover system requires regular maintenance.

5. The second ion gauge needs to be made to work.

6. Work needs to be done to understand the temperature control of the diffusion pumps. In particular, one of the pumps would not temperature stabilize at the end of the run. This problem must be solved. This may require vacuum-on time. If so, it must be scheduled during startup. Costs are uncertain, with a rough estimate of $5k to repair the stability problems.

4.12 Hall Dehumidifier Maintenance

The primary environmental control unit for the KTeV hall did not adequately control the humidity during the 1997 running period. During the summer months the hall relative humidity was as high as 80% at times. These high humidity levels exacerbated and triggered current draw problems in the drift chamber and TRD chamber systems. Reliable operation of the KTeV detector requires that the relative humidity in the hall remain below 50%. As a temporary measure during the high-humidity summer months, we rented an auxiliary air drying unit which proved to be inadequate. We intend to work with FESS to develop a strategy to fix this proplem.

5 Institutional Responsibilities

The institutional responsibilities for detector upgrades, commissioning, and maintenance during the 1999 run are listed in Table 23.

The Directorate has requested that we explicitly address the requirement for Fermilab postdoctoral researchers for the 1999 run. The Fermilab KTeV group currently is composed of five Research Associates and one Lederman fellow in addition to the senior staff. All of these postdoctoral researchers have now turned their focus toward analysis of the 1997 data set, and several will have moved on to new positions by the time of the 1999 run. The Fermilab KTeV group needs to replace at least two of the current postdoctoral researchers for the 1999 run in order to meet the institutional responsibilities listed in Table 23.

6 Cost, Manpower and Schedule Estimates

A breakdown of the cost estimates for the items described earlier appears in Table 24. The cost estimate is based on our experience in KTeV and does not include contingency or explicit manpower expenses. Considering the improvement over the 1997 run and the importance of the 1999 run for the ultimate success of the KAMI project, we believe these costs are well justified. In order to complete the required detector maintenance and modest upgrades in time for the run, timely funding is of critical importance. Significant funds for long lead-time maintenance must be made available in FY98.

Engineering and technical support will be required to complete the required maintenance and upgrades. The list of required Fermilab technical support can be found in Table 25. Technical support for replacement of the custom integrated circuits in the calorimeter readout system is the greatest immediate need, and the fabrication of the necessary parts is now in

Beam	FNAL
Vacuum	FNAL
Drift chambers and He bags	Chicago, Rice
CsI	Chicago, FNAL
Regenerator	Rutgers
Beam hole veto upgrades	UCLA
MA/PHV/SA/CIA/CA	Osaka,UCLA
V/V' system	Rutgers
Muon system	Rutgers
TRDs	Chicago, FNAL, Virginia
Beamline TRD	Chicago, FNAL
Level 1 & Level 2 trigger logic	Chicago
DC-or	Wisconsin
KQ/Banana	Colorado
Etotal/HCC	Arizona
TRD trigger	Virginia
STT trigger	Chicago, FNAL
YTF trigger	Chicago
FERA front-end readout	FNAL, Virginia
E832 Level 3 and monitoring	Arizona, Chicago
E799 Level 3 and monitoring	Colorado
DAQ	Arizona, Chicago, FNAL, Osaka, Wisconsin
Offline software	Arizona, Chicago

Table 23: Institutional detector responsibilities for the KTeV 1999 run.

progress. An important milestone is the replacement and recommissioning of the calorimeter readout system. This and other milestones are listed in Table 26.

We are currently considering several funding sources in addition to support from the lab. This includes DOE and NSF grants to each collaborating institution and funds from the US-Japan contract, provided through the Osaka University group.

Items	Cost	Subtotal
General repairs and upgrades		
QIE/DBC replacement	\$110k	
Chamber maintenance and repairs	\$45k	
Trigger/front end upgrades	\$35k	
Etotal repairs	\$12k	
DAQ system upgrade	\$219k	
		\$421k
Upgrades for $\pi^0\nu\overline{\nu}$		
Collimator for pencil beam	\$15k	
Beam hole veto	\$105k	
		\$120k
Upgrades for E-799 Hyperon Physics		
Beamline TRD	\$37k	
Move sweeper magnet upstream	\$5k	
		\$42k
Run maintenance and operating costs		
DLT tapes	\$150k	
Primary beam instrumentation	\$29k	
Chamber Gas	\$40k	
Calorimeter readout maintenance	\$5k	
CsI environmental control	\$5k	
Vacuum system maintenance	\$33k	
Hall dehumidifier maintenance	\$20k	
		\$282k
Total Cost		\$865k

Table 24: Capital cost projections for the 1999 run. Contingency and manpower costs are not included.

Items	Engineer Month	Technician Month
General repairs and upgrades		
QIE/DBC replacement	2	5
Chamber maintenance and repairs		8
Trigger/front end upgrades	1	2
Etotal repairs		2
DAQ (DART) system	30	6
Upgrades for $\pi^0\nu\overline{\nu}$		
Collimator for pencil beam	0.5	0.5
Beam hole veto	1	2
Upgrades for E-799 Hyperon Physics		
Beamline TRD	0.5	2
Move sweeper magnet upstream	0.5	0.5
Run maintenance and operating needs		
DLT tapes	NA	NA
Primary beam instrumentation	6	2
Chamber Gas	NA	NA
Calorimeter readout maintenance	0.5	1
CsI environmental control	0.5	0.5
Vacuum system maintenance	0.5	2
Hall dehumidifier maintenance	1	1
Total	44	34.5

Table 25: Fermilab engineering and technician requirements for the KTeV99 run. Manpower for rigging, alignment, radiation safety, as well as other normal operating technical support have not been included.

Date	Milestone
June 1997	Submission of Letter of Intent.
Sept. 1997	(End of FY97 run)
Dec. 1997	Submission of Proposal.
Jan. 1998	Pending approval, begin required detector maintenance.
April 1998	Establish technical feasibility of online splitting.
May 1998	Recommission calorimeter readout system.
June 1998	Restring radiation damaged drift chambers.
Oct. 1998	FY99, begin modest detector upgrade plan.
Jan. 1998	Begin commissioning of the KTeV detector.
April 1999	Begin data taking of FY99 run.

Table 26: Milestones for the KTeV 1999 run.

7 Possible Running Scenarios

To achieve the previously described physics goals in a twenty week run, we would allocate the following three blocks of running time:

1. 10 weeks of ϵ'/ϵ measurement;
2. 9 weeks of rare kaon decays;
3. 1 week of $K_L \to \pi^0\nu\overline{\nu}$.

During the 1997 data taking period the accelerator complex typically delivered 125-135 hours of beam per week to the KTeV experiment when all accelerator systems were operational. The physics program described in the previous sections is based on 8E12 protons per spill delivered to the KTeV experiment for 125 hours per week.

From the previous discussions of $K_L \to \pi^0\nu\overline{\nu}$ search issues and KAMI R&D, it is clear that detailed and careful background and detector studies are crucial for the eventual measurement of this process. To this end, we would allocate one week of $K_L \to \pi^0\nu\overline{\nu}$ running early and have this data set analyzed before the start of the rare kaon decay running. If the background level in the 1-week data set motivates more running, we would propose additional $\pi^0\nu\overline{\nu}$ running time.

Although the three physics programs in Table 27 nominally can be realized in a twenty week run, more running time would provide welcome insurance against unforseen losses. In particular, the proposed sensitivities rely on 125 hours of good beam per week which may be compromised by Main Injector or Tevatron commissioning.

	ϵ'/ϵ	Rare decays	$\pi^0\nu\bar{\nu}$
Proton Intensity	8E12	8E12	8E12
Beam size	9.3×9.3 cm^2	11.0×11.0 cm^2	4.0×4.0cm^2
No. of beams	2	2	1
Beam Absorber	In	Out	In
Mask Anti	In	Out	In
Regenerator	In	Out	Out
Running time	10 weeks	9 weeks	1 week
Improvement(KTeV97+KTeV99)	KTeV97 $\times 2$	KTeV97 $\times 3$	KTeV97 $\times 16$
Sensitivity (KTeV97+KTeV99)	$\sigma_{stat} =$ 1.0×10^{-4}	SES = 10^{-11} regime	SES = 2.5×10^{-8}

Table 27: Conditions for the three running periods in 1999.

8 Conclusion

Although KTeV's first run was successful and will produce many significant physics results, we believe we have only begun to exploit the physics potential of this state-of-the-art detector. The 1999 run provides us with the opportunity to continue this program to meet and perhaps exceed our original goals for both E832 and E799. As discussed in this proposal, the few problems encountered during the KTeV97 run are being addressed, so that the 1999 data sample should have better systematic properties than the 1997 data. As the offline analysis proceeds, we will continue to learn how to take better data in 1999.

The 1999 run will also allow us to continue to investigate the $K_L \rightarrow \pi^0\nu\bar{\nu}$ decay. Experience gained in the 1999 run will be an important and necessary step towards a program to detect and measure this mode in KAMI.

In summary, 20 weeks of additional running in 1999 will allow KTeV to address the three areas of greatest interest in kaon physics with unprecedented sensitivity:

1. measure ϵ'/ϵ with an accuracy of 1×10^{-4} (E832) ;

2. search for and study rare decays to sensitivities near 10^{-11} (E799);

3. continue our studies of $K_L \rightarrow \pi^0\nu\bar{\nu}$, which will include the first KAMI prototype detectors operating in a realistic beam environment.

We also propose to continue our program of hyperon physics which has already produced a number of interesting results.

We believe the proposed program will make the best use of a 20 week run. It should be noted that this running period includes no time for detector commissioning, and assumes 125 hours of good beam per week. It seems likely that more than 20 calendar weeks will be required to collect the data samples described in this proposal. While this group eventually expects to do excellent physics using 120 GeV beam from the Main Injector, it should be noted that the KTeV detector is currently optimized for 800 GeV beam. Since the 1999 fixed-target run will be the last at 800 GeV, we believe it is important to collect enough data during 1999 to complete the physics goals described above.

9 Acknowledgments

The success of KTeV to this point is in large part due to the tremendous effort expended by many physicists, graduate students, engineers, and technicians. Many of these people will not be involved directly in the 1999 run, but their contributions to KTeV will be felt in 1999 and beyond.

Particularly noteworthy have been the contributions of the following people: C. Bown, C. Qiao and P. Shawhan from the University of Chicago, P. Mikelsons and U. Nauenberg of the University of Colorado, P. Johnson, T. Nakaya and D. Pushka of Fermilab, J. Kubic, J. Jennings and S. Field of UCLA; H. Kobrak of U.C. San Diego; and A.P. McManus of the University of Virginia.

A $K_L \to \pi^0 \nu \overline{\nu}$ Background Studies

The backgrounds to $K_L \to \pi^0 \nu \overline{\nu}$ from K_L and Λ decays are described below.

A.1 $K_L \to \pi^0 \pi^0$

A total of 110 million events were generated in this mode, with the kaon momentum in the range $10 < p < 310$ GeV/c, and the Z position of the decay vertex in the range $90 < Z < 180$ m. After the final cuts, 37 events end up in the signal region ($160 < P_T < 300$ MeV/c).

Figure 16(a) shows the P_T distribution of these events, and Figure 16(b) shows the ΔZ distribution, where ΔZ is the difference between the reconstructed and the generated Z positions of the decay vertex. The majority of the events are clustered near $\Delta Z = 0$. These events originate from an even-combination of the photons, that is, where both the photons come from the same π^0 so that the decay vertex is reconstructed correctly. These are problem events, because even if one were to determine the Z position of the decay vertex independently (e.g. using a gamma converter), these events will pass all of the cuts. There are four events which have large ΔZ's. These originate from so-called odd-combinations of photons, in which the two photons did not come from the same π^0. These events can in principle can be rejected, for example, by using a gamma converter, but they are only a small fraction of the total number of events. One could reduce this background by applying a tighter P_T cut (say $P_T < 190$ MeV/c, see Figure 16(a)), but that would result in a significant loss of the signal.

Figure 16(c) shows the E_T distribution for these events, where E_T is the total energy deposited in the calorimeter. Most of the events are clustered at low E_T. After requiring that $E_T > 15$ GeV, only one event remains. This turns out to be a good cut, since it keeps 80% of the $\pi^0 \nu \overline{\nu}$ signal which remains after all other final cuts (see Figure 16(d)). The background level is defined as:

$$\mathrm{BL} = \frac{N_{obs}}{N_{K_L}^{gen}} \times \frac{BR(K_L \to \pi^0\pi^0)}{\epsilon_{\pi^0\nu\overline{\nu}}} \tag{1}$$

where N_{obs} is the number of events from $K_L \to \pi^0\pi^0$ observed in the signal region after final cuts, $N_{K_L}^{gen}$ is the total number of generated K_L decays in the Monte Carlo, and $\epsilon_{\pi^0\nu\overline{\nu}}$ is the acceptance for the $\pi^0\nu\overline{\nu}$ signal after final cuts.

After applying the cut ($E_T > 15$ GeV), the background level from the $K_L \to \pi^0\pi^0$ mode is:

$$\mathrm{BL}_{2\pi^0} \simeq \frac{1}{11 \times 10^7} \times \frac{9 \times 10^{-4}}{0.0125} = 6.5 \times 10^{-10} \tag{2}$$

where the factor 0.0125 in the denominator is the acceptance for the signal generated in the decay region $90 < Z < 180$ m, after the final cuts, including the cut $E_T > 15$ GeV.

A.2 $K_L \to \pi^0\pi^0\pi^0$

From a total of 2.6×10^9 generated events ($10 < p < 310$ GeV/c and $90 < Z < 180$ m), five events pass all the cuts and end up in the signal search region ($160 < P_T < 260$ MeV/c). Figure 17(a) shows the P_T distribution of these remaining events. Figure 17(b) shows the reconstructed vs. generated Z position of the decay vertex, and Figure 17(c) is the ΔZ distribution for these events. Clearly, these are all 'odd' combinations of photons. Figure 17(c) shows the distribution of the total deposited energy, E_T, in the calorimeter. One event remains after the cut $E_T > 15$ GeV/c. This corresponds to a background level of:

$$\mathrm{BL}_{3\pi^0} \simeq \frac{1}{2.6 \times 10^9} \times \frac{0.21}{0.0125} = 6.5 \times 10^{-9}. \tag{3}$$

In the letter of intent for KTeV99, we had mentioned that it might be necessary to build another Mask Anti (MA) photon veto detector upstream of the existing one to suppress upstream $3\pi^0$ events. In a Monte Carlo simulation, we generated $3\pi^0$ events upstream of the existing MA ($90 < z < 120$ m) up to a single event sensitivity of 3×10^{-9}. None of the events passed the final selection criteria. As a result, we conclude that an additional upstream MA will not be required to achieve the proposed sensitivity during KTeV99.

A.3 $K_L \to \gamma\gamma$

This decay mode is a source of background only if one of the photons is missed and another accidental photon combines with the remaining one to give rise to a high P_T. Out of a total of 41.3 million generated decays in this mode, none pass the final selection criteria. This translates into a background level of

$$\mathrm{BL}_{2\gamma} < \frac{1}{41.3 \times 10^6} \frac{5.9 \times 10^{-4}}{0.0125} = 1.1 \times 10^{-9}. \tag{4}$$

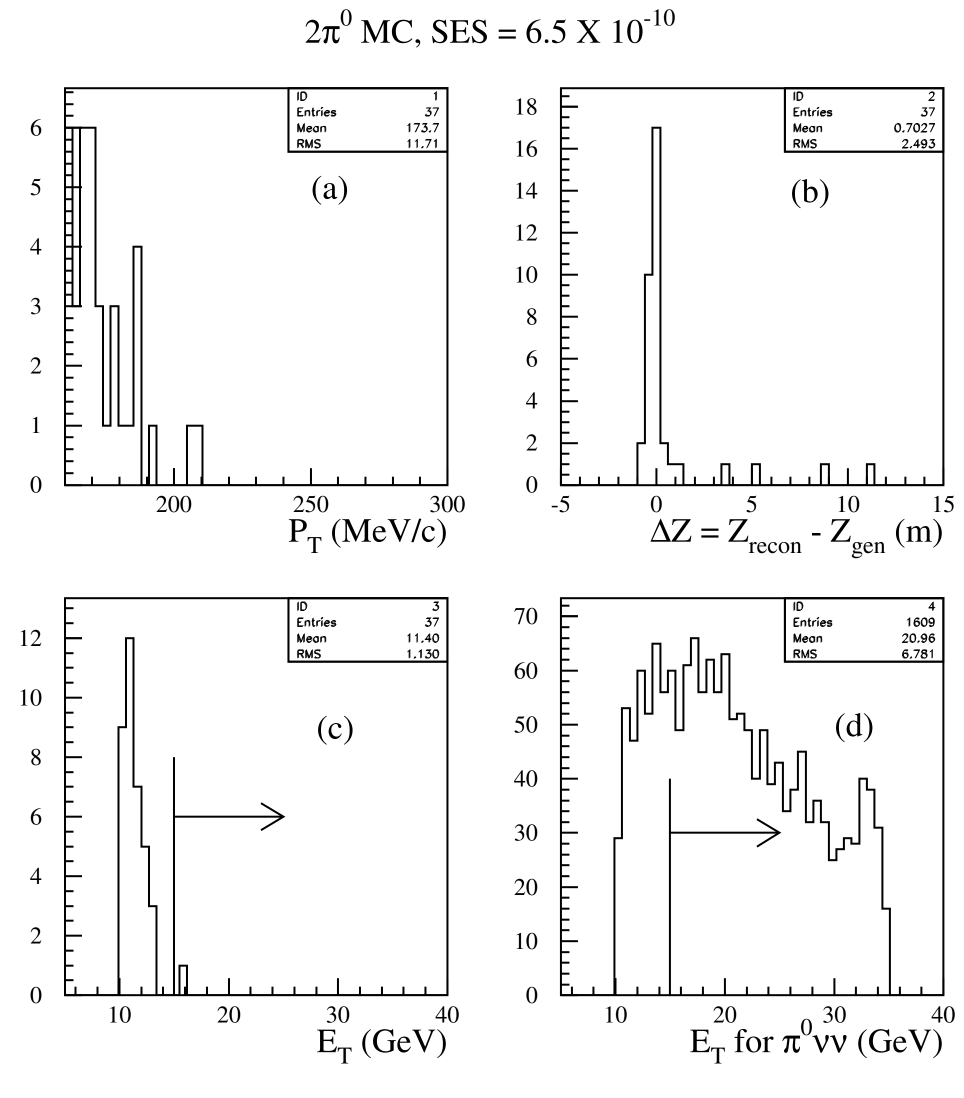

Figure 16: Some distributions for Monte Carlo generated $K_L \to \pi^0\pi^0$ background events in the $K_L \to \pi^0\nu\overline{\nu}$ signal region which pass the final cuts, as described in the text. Figure (a) shows the P_T distribution, and (b) is the ΔZ distribution, where ΔZ is the difference between the reconstructed and the generated Z decay positions. Figure (c) shows the total energy deposited in the calorimeter by these events, and (d) is the same quantity for the $\pi^0\nu\overline{\nu}$ signal mode. $E_T > 15$ GeV gets rid of almost all of $2\pi^0$ background events, while keeping 82% of the signal.

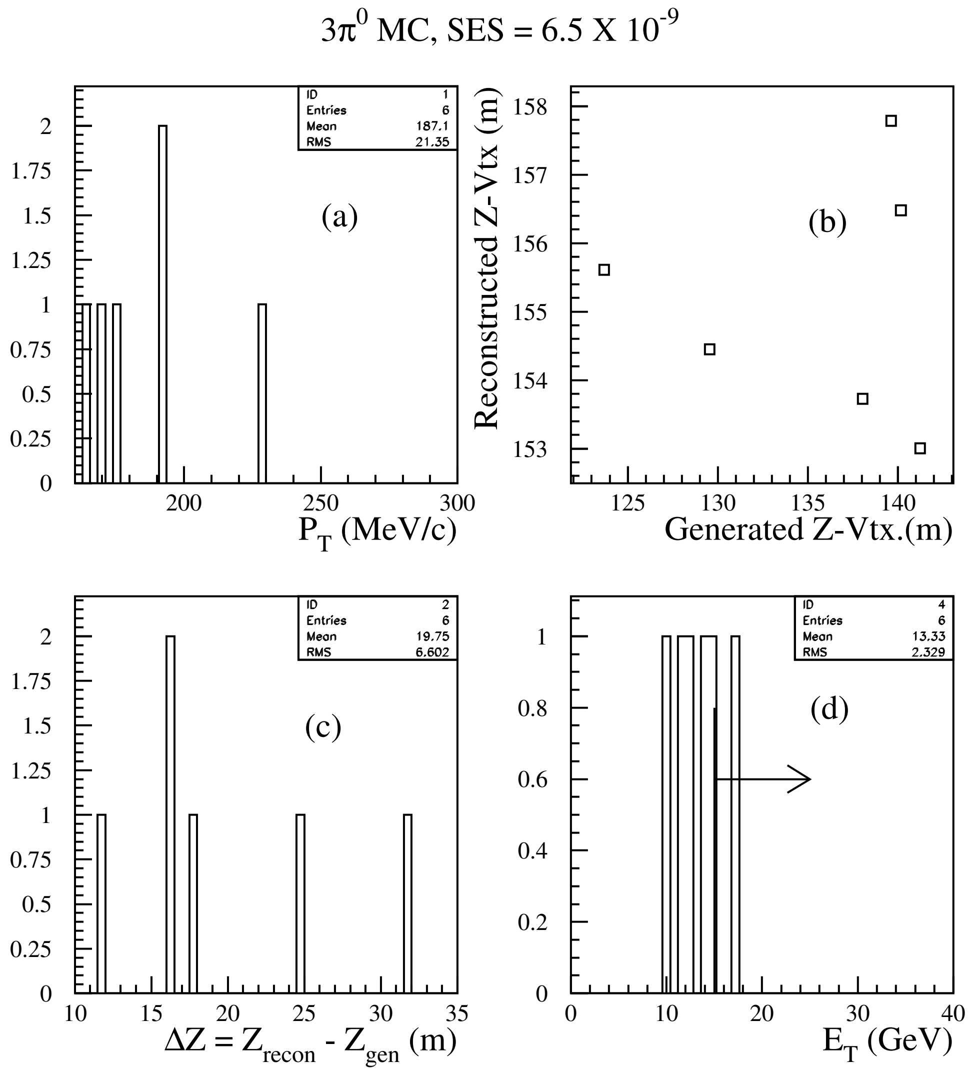

Figure 17: Some distributions from the $3\pi^0$ Monte-Carlo simulation: (a) The P_T distribution, (b) The reconstructed vs. generated Z positions of the decay vertex, (c) ΔZ, the difference between the reconstructed and the generated Z positions of the decay vertex, and (d) The distribution of the total deposited energy in the calorimeter.

A.4 $\Lambda \to n\pi^0$

High momentum Λ decays in the fiducial region of the detector can appear as a background if the neutron goes undetected. To study this background, events were generated in the momentum range $40 < p < 500$ GeV/c. Out of a total of 21 million generated decays, 8 survive the final cuts, ending up in the signal search window $160 < P_T < 260$ MeV/c. Figure 18(a) shows the P_T distribution of these events. As can be seen from Figures 18(b) and 18(c), these are all odd-combination events, as expected, since an even combination will result in the correct P_T. Figure 18(d) shows the E_T distribution for such events. The cut $E_T > 15$ GeV/c does not remove any of these events. The background level from these decays is:

$$\mathrm{BL}_{\Lambda \to n\pi^0} = \frac{N_\Lambda}{N_{K_L}} \times \frac{N^{obs}_{n\pi^0}}{N^{gen}_{n\pi^0}} \times \frac{BR(\Lambda \to n\pi^0)}{\epsilon_{\pi^0\nu\overline{\nu}}} \tag{5}$$

where N_Λ/N_{K_L} is the ratio of the number of Λ's to that of K_L's in the beam, $N^{obs}_{n\pi^0}$ is the number of observed $\Lambda \to n\pi^0$ events after the final cuts, and $N^{gen}_{n\pi^0}$ is the total number of generated $\Lambda \to n\pi^0$ events. In the KTeV beam, under conditions which correspond to the one day special $\pi^0\nu\overline{\nu}$ run, the Λ to K_L ratio is, approximately,

$$\frac{N_\Lambda}{N_{K_L}} \simeq \frac{1}{100} \tag{6}$$

The background level from Λ decays is then

$$\mathrm{BL}_{\Lambda \to n\pi^0} = \frac{1}{100} \times \frac{8}{21 \times 10^6} \times \frac{0.36}{0.0125} = 1.1 \times 10^{-7}. \tag{7}$$

However, this background level is overestimated! The reason is that in the existing Monte Carlo, the hadronic interactions in the beam hole veto are not modeled. As a result, even if the neutron from the decay goes down the beam hole, it is not vetoed in the Monte Carlo, even though it would be vetoed with some efficiency by the beam hole veto in reality. Figure 19 shows the effect of the beam hole veto on Λ decays in the data. The solid line is the P_T distribution of the events without the beam hole veto, and the dashed line is the same distribution after the beam hole veto cut. The peak around $P_T = 100$ MeV/c is due to the $\Lambda \to n\pi^0$ decays. Clearly, this peak goes down by about a factor of 5 when the beam hole veto cut is applied. This is consistent with hadron rejection which is approximately 80% efficient.

Figure 20(a) shows the Y positions of the neutrons from Λ decays at the CsI calorimeter. The beam hole is indicated by the region between the vertical lines. Clearly, all the neutrons go down the beam hole. This is not surprising, since these are all very high energy neutrons (see Figure 20(b)). We plan to build a new hadronic beam hole detector (see Section 4.7.2), which would veto neutrons with a 99% efficiency. If this factor is taken into account, then the background level from the Λ decays reduces to:

$$\mathrm{BL}_{\Lambda \to n\pi^0} = 1.1 \times 10^{-7} \times (0.01) = 1.1 \times 10^{-9} \tag{8}$$

where the factor of 0.01 is for the neutron rejection we expect to achieve with the new hadronic beam hole detector.

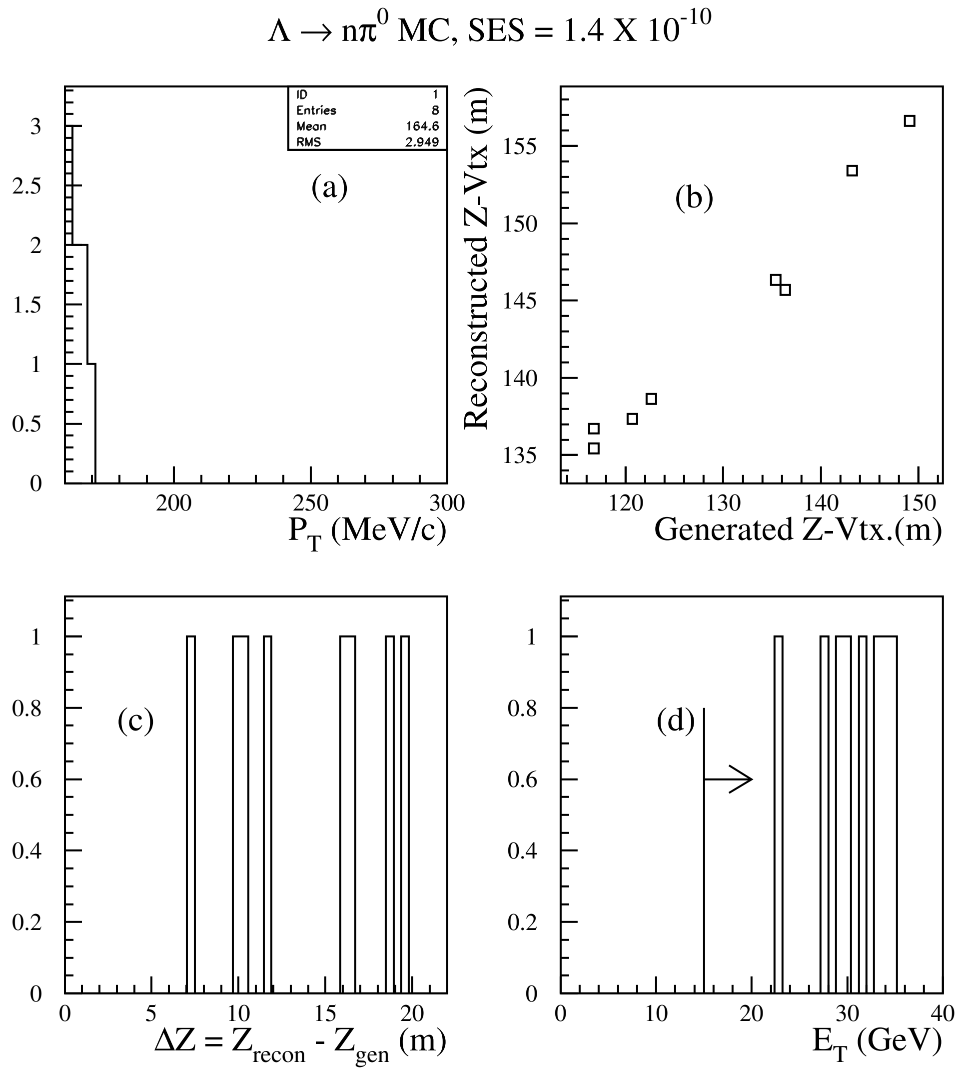

Figure 18: The Monte Carlo generated P_T, Z, ΔZ and E_T distributions for $\Lambda \rightarrow n\pi^0$ decays.

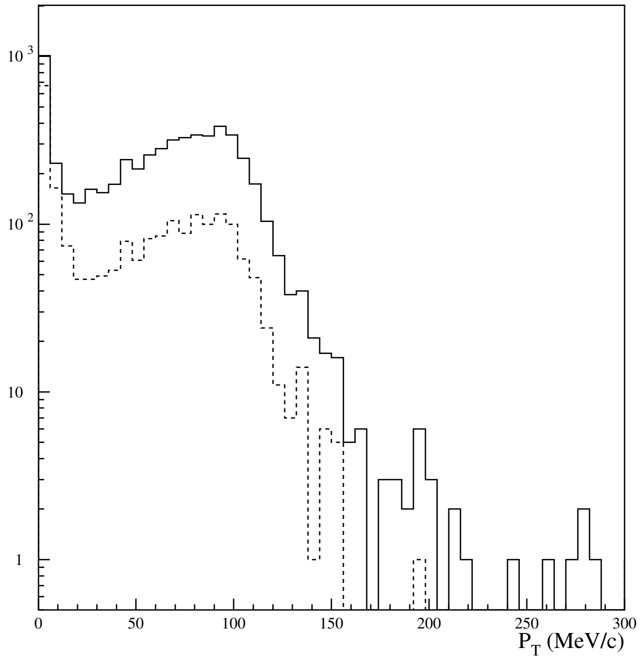

Figure 19: The P_T distribution of two-cluster events in the data from the $K_L \rightarrow \pi^0 \nu \overline{\nu}$ decay search before (solid line) and after (dashed line) the beam hole veto cut. The peak around $P_T = 100$ is mainly due to the decay $\Lambda \rightarrow n\pi^0$. The beam hole veto cut clearly rejects these event by vetoing the neutron interactions.

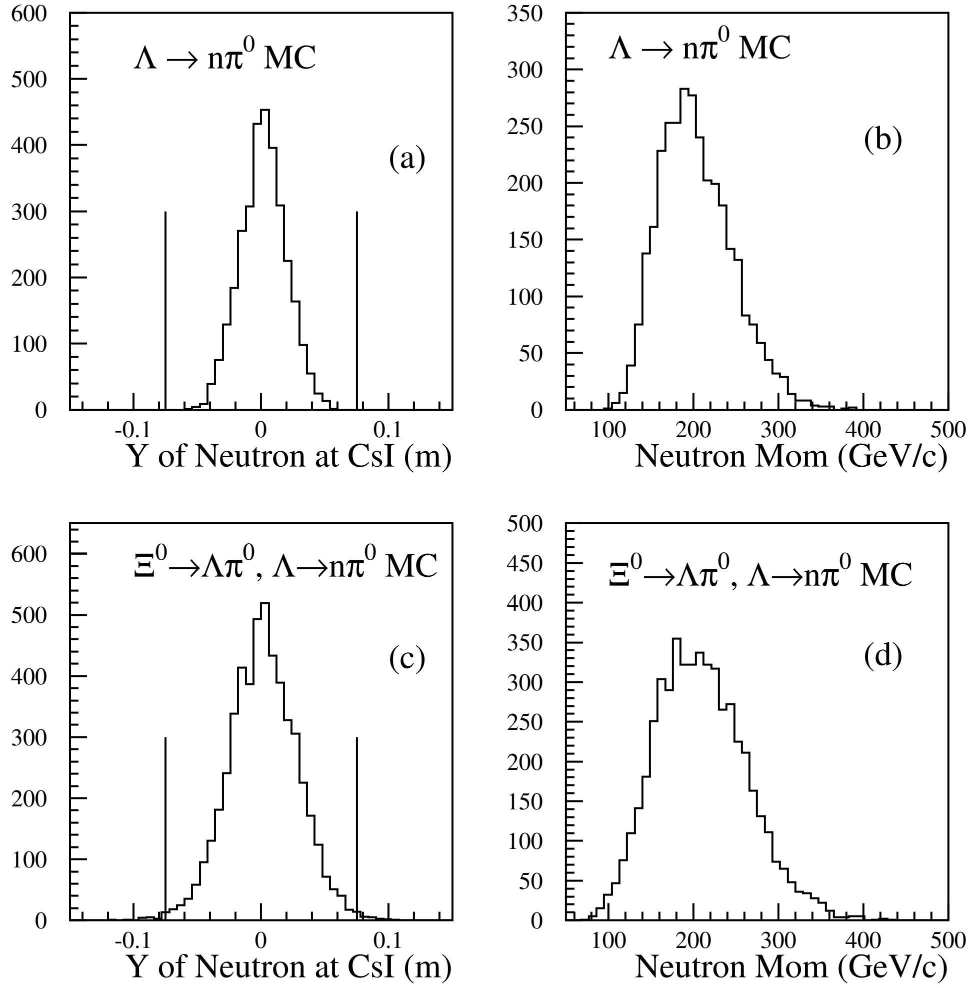

Figure 20: The Y positions (a and c) at the CsI, and the momentum spectra (b and d) of the neutron from Monte Carlo generated Λ and $\Xi^0 - \Lambda$ decays. The region between the vertical lines in (a) and (c) is the beam hole. Nearly all the neutrons go down the beam hole, since they have very high energies.

A.5 $\Xi^0 \to \Lambda\pi^0$

We generated 16 million events of the type $\Xi \to \Lambda\pi^0$ followed by the decay $\Lambda \to n\pi^0$. 13 of these events pass the final selection criteria and appear in the signal search region, $160 < P_T < 260$ MeV/c. The P_T distribution for these events is shown in Figure 21(a). Figure 21(b) shows the reconstructed vs. the generated Z position of the decay vertex, and Figure 21(c) shows the ΔZ (defined previously) distribution. Both even and odd combinations are visible and contribute in this mode, since an accidental photon is not necessarily required to give rise to a large P_T. Figure 21(c) shows the E_T distribution for these events. The cut $E_T > 15$ GeV does not remove any of these events. The background level corresponding to these events is:

$$\mathrm{BL}_{\Xi^0} = \frac{N_{\Xi^0}}{N_{K_L}} \times \frac{N^{obs}_{n\pi^0}}{N^{gen}_{\Xi^0}} \times \frac{BR(\Lambda \to n\pi^0)}{\epsilon_{\pi^0\nu\overline{\nu}}} \tag{9}$$

where N_{Ξ^0}/N_{K_L} is the ratio of the number of Ξ^0 to that of K_L in the beam, which was estimated to be (at KTeV97):

$$\frac{N_{\Xi^0}}{N_{K_L}} \simeq \frac{1}{2400}. \tag{10}$$

Therefore, the background level from this decay mode is:

$$\mathrm{BL}_{\Xi^0} = \frac{1}{2400} \times \frac{13}{16 \times 10^6} \times \frac{0.36}{0.0125} = 9.7 \times 10^{-9}. \tag{11}$$

Again, this background estimate does not include any rejection power from the beam hole veto. Figure 20(c) shows the Y position of the neutrons from the $\Xi - \Lambda$ decay chain, and Figure 20(d) shows the momentum spectrum of these neutrons. Nearly all of these neutrons go down the beam hole. Clearly, these neutrons can be vetoed with a hadronic beam hole veto. Again, assuming 99% efficient neutron rejection, we get:

$$\mathrm{BL}_{\Xi^0} = (9.7 \times 10^{-9}) \times (0.01) = 9.7 \times 10^{-11}. \tag{12}$$

B A γ-converter for $K_L \to \pi^0\nu\overline{\nu}$ detection

We performed an extensive study of the possibility of using a γ converter to measure $K_L \to \pi^0\nu\overline{\nu}$ decays in KTeV99. Figure 22 shows the final signal acceptance for different thicknesses for the Pb converter and for three different P_T kicks in the magnet which were considered. Clearly, a P_T kick of 100 MeV and Pb thickness of 1 mm (0.18 X_0) are near optimum. A P_T kick of 50 MeV gives a little better acceptance, but the E/p resolution is worse. A P_T kick of 200 MeV will give better E/p resolution, but the acceptance drops by approximately a factor of 2, due to low energy conversion electrons bending out of the acceptance. A thicker lead plate results in more γ-conversions, but it also results in more energy loss by the converted e^+e^- pair via bremsstrahlung. Therefore, more electrons (or positrons) will bend out of the acceptance. Also, bremsstrahlung results in additional clusters in the calorimeter, therefore reducing efficiency, since we demand exactly three clusters (one from the unconverted photon, two from the conversion pair) in the calorimeter. One

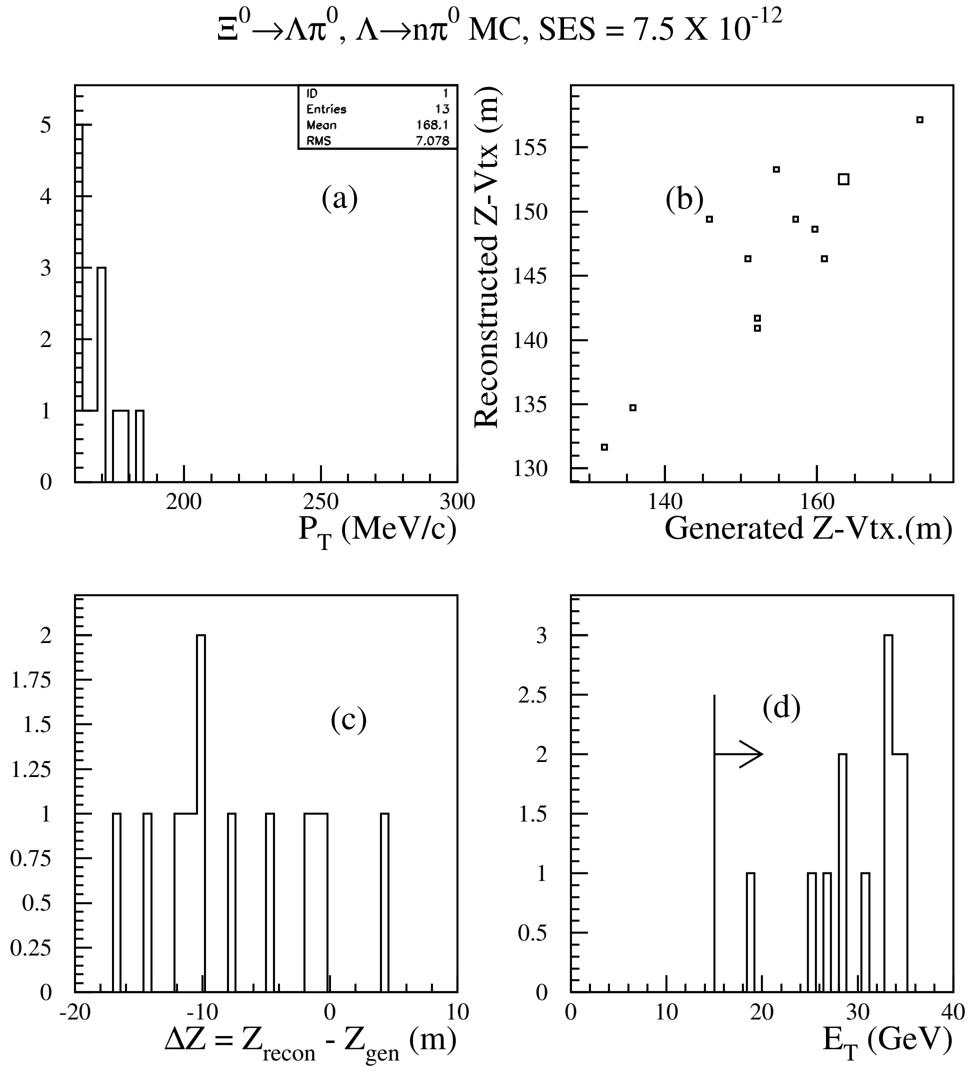

Figure 21: The Monte Carlo generated P_T, Z, ΔZ , and E_T distributions for $\Lambda \rightarrow n\pi^0$ decays, where the Λ originates from a Ξ^0 decay.

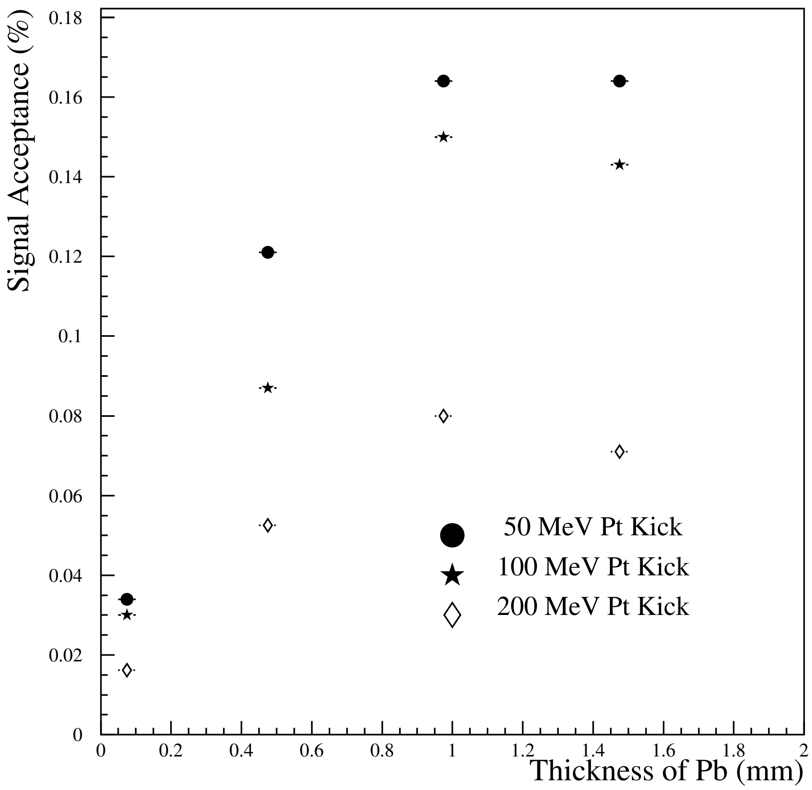

Figure 22: The $\pi^0\nu\overline{\nu}$ signal acceptance using a γ-converter for various thicknesses of lead and various magnet P_T kicks when at least one of the photons is converted into e^+e^- pair.

can, in principle, allow for more than three clusters, but that would also result in admitting more background. For example, if one allows for four clusters in the calorimeter, then only one photon from a $2\pi^0$ decay needs to escape detection in order for this event to appear as background. Table 28 lists the achievable sensitivity per/week with a 1 mm thick lead converter and a 100 MeV P_T kick for various running conditions.

Clearly, the SES/week achievable by using a gamma-converter is too small to be attractive. Using a small beam with an absorber, we don't accumulate sufficient statistics. With bigger beams, we start to lose signal due to accidental activity, since we have to cut very tightly on photon veto detectors. For example, for a 6×6 cm^2 beam without absorber, the signal loss is very large. Therefore, even though we gain in the kaon flux by taking the beam absorber out, the much increased accidental activity and neutron flux cause us to lose signal acceptance. The detector most affected by the increased neutron flux is the beam hole veto.

Since the additional sensitivity which results from adding a γ-converter is minimal, we have decided to abandon this idea for the KTeV99 run.

Running Condition	Signal Eff.	SES/Week
4×4 cm^2 beam, Absorber IN	0.15%	3×10^{-7}
6×6 cm^2 beam, Absorber IN	0.10%	2×10^{-7}
6×6 cm^2 beam, Absorber OUT	0.04%	3×10^{-7}

Table 28: The Expected single event sensitivity (SES) for $K_L \to \pi^0\nu\overline{\nu}$ at KTeV99 using a 1 mm Pb (0.18 X_0) γ-converter for various running conditions.

C Measurement of photon veto inefficiency at KEK-INS for KAMI

Obtaining an accurate understanding of our photon detection capabilities is of critical importance in order to proceed with our program to measure $K_L \to \pi^0\nu\overline{\nu}$ at KAMI. We have started a collaboration with a Japanese group to carry out a beam test at INS (Institute of Nuclear Study) in Japan.

One of the photon energy regions where we need to understand the photon detection inefficiency rather well is between 100 MeV and 1 GeV. In this region, the inefficiency is dominated by photonuclear absorption. The cross section, and thus the inefficiency, increases with photon energy, although the detection probability of secondary pions which may be produced also increases with energy. Due to such competing effects, the inefficiency should be measured experimentally.

Dr. Inagaki and his group (INS ES147) have established a method to tag a photonuclear interaction by using a tagged photon beam combined with neutron detection to tag neutrons resulting from the interaction. In their previous experiment, they seem to have achieved a sensitivity of $< O(10^{-5})$, though this is still very preliminary.

We are now collaborating with Inagaki to perform a new measurement at KEK-INS in the spring of 1998. The goal of this effort is to measure the photon detection inefficiency of KTeV's pure CsI crystals and a new prototype photon veto detector. We plan to improve the coverage of the neutron counters, use FADCs to read out the neutron counters for better neutron ID, improve the data acquisition rate for higher statistics, and improve the beamline. Osaka University, UCLA, The University of Chicago, and Fermilab are currently planning to represent KTeV/KAMI in this effort. This test should give us a much better understanding of the features and limitations of photon veto detectors and will allow us to plan much more effectively for KAMI.

References

[1] B. Winstein and L. Wolfenstein, Rev. Mod. Phys. **65**, 1113 (1993).

[2] L. K. Gibbons *et al.*, Phys. Rev. Lett. **70**, 1203 (1993).

[3] G. D. Barr *et al.*, Phys. Lett. **B317**, 223 (1993).

[4] J.L. Ritchie and S.G. Wojcicki, Rev. Mod. Phys. **65**, 1149 (1993) and references within.

[5] G. Buchalla and A.J. Buras, Phys. Rev. **D54**, 6782 (1996).

[6] A. J. Buras, hep-ph/9609324, September 1996 (to appear in "Workshop on K-Physics", Orsay, May 1996).

[7] A. J. Buras and R. Fleischer, hep-ph/9704376, April 1997 (To appear in "Heavy Flavors II", World Scientific, 1997).

[8] K. Arisaka *et al.*, KTeV Design Report: Fermilab Report FN-580 (Jan., 1992).

[9] L.M.Sehgal and M.Wanninger, Phys. Rev. **D46**, 1035 (1992); also P. Heiliger and L.M.Sehgal, Phys. Rev. **D48**, 4146 (1993).

[10] H.B. Greenlee, Phys. Rev. D **42**, 3724 (1990).

[11] D. A. Harris *et al.*, Phys. Rev. Lett. **71**, 3918 (1993).

[12] V. O'Dell, KTeV Collaboration, "Status and New Results of the KTeV Rare Kaon Program," MIST Workshop Fermilab,(May,1997) to be published.

[13] E. J. Ramberg, Fermilab-Conf-91/258, (1991); E. J. Ramberg, *et al.* Phys. Rev. Lett. **70**, 2529 (1993).

[14] T. Nakaya, Flavor Changing Neutral Current Conference, Santa Monica, CA (1997).

[15] M. Weaver *et al.*, Phys. Rev. Lett. **72**, 3758 (1994).

[16] A. Manohar and A. Garcia, private communication; also see J. Dai *et al.*, Phys. Rev. **D53**, 273 (1996).

[17] J. Lach and P. Zenczykowski, Int. J. of Mod. Phys. **A10**, 3817 (1995).

[18] J. L. Rosner, "Improved Tests of Relations for Baryon Isomultiplet Splittings", EFI 97-33, hep-ph/9707473, (July, 1997), submitted to Phys. Rev. D.

[19] G.R. Farrar, Phys. Rev. Lett. **76**, 4111 (1996).

[20] G.R. Farrar, Phys. Rev. Lett. **76**, 4115 (1996).

[21] J.Adams *et al.*, Phys. Rev. Lett. **79**, 4083 (1997).

[22] K. Arisaka *et al.*, "Conceptual Design Report: Kaons at the Main Injector," Fermilab Report FN-568 (June, 1991).

[23] E. Cheu *et al.*, "An Expression of Interest to Detect and Measure the Direct CP Violating Decay $K_L \rightarrow \pi^0 \nu\overline{\nu}$ and Other Rare Decays at Fermilab Using the Main Injector," Fermilab-Pub-97-321-E.

[24] D. A. Harris *et al.*, Phys. Rev. Rett. **71**, 3914 (1993).

[25] P. Gu, *et al.* Phys. Rev. Rett. **72**, 3758 (1993).

[26] P. Gu, *et al.* Phys. Rev. Rett. **76**, 4312 (1996).

[27] N. Samios, Phys. Phys. Rev. **126**, 1844 (1962).

[28] A. Deshpande *et al.*, Phys. Rev. Lett **71**, 27 (1993).

[29] K. McFarland *et al.*, Phys. Rev. Lett. **71**, 31 (1993).

[30] BNL E845, Phys. Rev. Lett. **65**, 1407 (1990).

[31] CERN NA31, Phys. Lett. **B240**, 283 (1990).

[32] T. Nakaya, *et al.* Phys. Rev. Rett. **73**, 2169 (1994).

[33] M. Spencer, *et al.* Phys. Rev. Rett. **74**, 3323 (1994).

[34] S. Teige *et al.*, Phys. Rev. Lett. **63**, 2717 (1989).

[35] C. James *et al.*, Phys. Rev. Lett. **64**, 843 (1990).

[36] S. Y. Hsueh *et al.*, Phys. Rev. **D38**, 2056 (1988).

[37] A. Garcia and P. Kielanowski, "The Beta Decay of Hyperons" (Lecture Notes in Physics, vol. 222), Springer-Verlag (1985).

[38] N. Solomey *et al.*, Nucl. Inst. Meth. **A367**, 252 (1995).

[39] V. O'Dell, T. Yamanaka, "The KTeV Data Acquisition System", KTeV internal note # 184.

[40] T. Alexopoulos *et al.*, "Proposed Design of the KTeV Slow-DAQ", KTeV internal note # 256.

[41] D. Errede *et al.*, Nucl. Inst. Meth. **A309**, 386 (1991).

[42] H. Fenker, "A Standard Beam PWC for Fermilab", Fermilab Report TM-1179 (February, 1983).